An Interface for Analysis of Medical Linear Accelerator Performance Parameters Using Process Behavior Charts

BY

Callistus I Huy Minh Nguyen

A Thesis Submitted to the Graduate Faculty of

VIRGINIA TECH – WAKE FOREST UNIVERSITY

SCHOOL OF BIOMEDICAL ENGINEERING & SCIENCES

In Partial Fulfillment of the Requirements

for the Degree of

MASTER OF SCIENCE

Biomedical Engineering

December 2014

Winston-Salem, North Carolina

Approved by:

Michael T. Munley, PhD, Advisor, Chair

Examining Committee:

Craig A. Hamilton, PhD

Charles M. Able, MS

ACKNOWLEDGEMENTS

I would like to thank my co-advisor, Mr. Charles M. Able for his guidance throughout my thesis work and other projects. I have been challenged on a daily basis and am grateful for the experiences that I have received thus far. You have helped me grow as a researcher and taught me a number of things about being a medical physicist. I am very thankful to have worked with you during my time in the Radiation Oncology department and look forward to working with you during the next phase of your career.

I would also like to thank of advisor, Dr. Michael T. Munley, for allowing me the opportunity to be a part of the Radiation Oncology department. I am grateful for the number of opportunities to grow, not only as a person, but as a scientist in the medical field. I would also like to thank the rest of my committee, Dr. Craig Hamilton. Dr. Hamilton has been a great resource for all MATLAB programming and I am very thankful to have him share his knowledge.

Finally, I would like to thank my family and friends for all their support during my academic career.

TABLE OF CONTENTS

ACKNOWLEDGEMENTS ..... **ii**

TABLE OF CONTENTS ..... **iii**

LIST OF TABLES ..... **v**

LIST OF FIGURES ..... **vi**

ABBREVIATIONS ..... **ix**

ABSTRACT ..... **xi**

I. Introduction **1**

a. Description of a Linear Accelerator and its Components 3

b. System Interlocks 16

c. Current Maintenance Procedures and the Impact of System Downtime 17

II. Statistical Process Control and Its Uses **18**

a. General Information 18

b. Techniques: Xbar/R and I/MR Charts 18

c. Previous work of the use of SPC on Linear Accelerators 23

SPC used in accelerator performance and reliability 23

III. Predictive Maintenance Model for Medical Linear Accelerators **26**

a. Daily QA Treatment Delivery and File Transfer 27

b. File Decoding, Data Analysis and Regrouping 27

c. SPC Analytical Formulism and Evaluation Guidelines 28

d. Database Design 31

IV. Interface Development and Use **37**

V. PdM Effectiveness and Operational Consistency **53**

a. System Dysfunction Detection and Confirmation 53

Beam Uniformity 53

Gantry Position Accuracy 54

MLC Motor 55

b. Operational Consistency 57

VI. Conclusion **74**

a. PMD Effectiveness as a PdM Tool 74
b. PdM Reliability in Predicting Component Failure 74
c. Uniqueness of Linear Accelerator Performance 75
d. Limitations 75
e. Future 76
VII. References 77
VIII. Scholastic Vita 79

LIST OF TABLES

Table I: Bending Magnet Systems 13
Table II: MATLAB GUI Components 38
Table III: MATLAB Figure Properties 38
Table IV: MATLAB Axes Properties 39
Table V: MATLAB uicontrols 40
Table VI: MATLAB uicontrols Properties 41
Table VII: Statistics for Important Performance Parameters in TrueBeam systems (7 linear accelerators – TB and STX models) 58
Table VIII: Statistics for Important Performance Parameters in TrueBeam systems (4 linear accelerators – STX Models) 59
Table IX: Statistics for Important Performance Parameters in TrueBeam systems (2 linear accelerators – STX consecutive serial numbers) 59

LIST OF FIGURES

Figure 1. A basic schematic of a medical linear accelerator [8]. 4
Figure 2. A cross-sectional drawing of a magnetron. E_p represents the pulsed electric field and E_m represents the microwaves. S represents the path the electrons take under the influence of a magnetic field [6]. 6
Figure 3. (a) A cross-sectional drawing of a two-cavity klystron tube used as a microwave amplifier. (b) The electric field varies sinusoidally in the first or buncher cavity [6]. 7
Figure 4. (a) Travelling wave accelerating waveguide. (b) Standing wave accelerating waveguide [8]..... 10
Figure 5. Auxiliary components of a medical linear accelerator system [6]. 14
Figure 6. A basic schematic of an Xbar/R chart. 20
Figure 7. A basic schematic of an I/MR chart. 22
Figure 8. Normal probability density functions representing three I chart limit calculation methods for 6 MV photon transverse symmetry: traditional/standard SPC, symmetry specification (±2%), and our hybrid method that includes the standard SPC calculation and an empirical factor (S_p). 30
Figure 9. The main GUI window of the PMD. It houses all of the components necessary to develop a PdM system for medical linear accelerators. The PMD has three initial options: File, View, and Machines. 44
Figure 10. Loading the data into the PMD. The PMD requires two data matrices: machinedata.mat and SPC_MachineName.mat. (a) A window loads and asks the user to locate machinedata.mat (b) A window loads immediately after and asks the user to locate SPC_MachineName.mat..... 45
Figure 11. (a) First set of pushbuttons that is seen. These are the nine major categories that contain all of the performance parameters. The operating status is adjacent to the pushbutton. (b) Each pushbutton has a callback that initiates a second set of pushbuttons that contain the specified performance parameter. In this case, these performance parameter pushbuttons correspond to RF Generation. 48
Figure 12. An I/MR chart is generated based on the specified performance parameter. Red lines indicate the chart control limits while the white line indicates the grand mean. A horizontal frequency distribution is generated in parallel with the individual data set distribution. Other features generated by GRAPH.M are also seen. 49
Figure 13. The 'Apply New Baseline' feature that is provided by the PMD. 50
Figure 14. The 'Add Comments' feature that is provided by the PMD..... 51
Figure 15. Each MLC leaf has its own pushbutton that allows for rapid interrogation. 52
Figure 16. The progress of the ARC at one of our DCP facilities. Continuous monitoring following service adjustments indicates beam steering was restored to its baseline value. 54

Figure 17. The progress of the GLCC at one of our DCP facilities. New chart control limits needed to be revised when the process operated at a new baseline value. 55
Figure 18. The progress of the CC Max Values of MLC Leaf 26 in carriage bank B. PdM monitoring revealed that the process was deviating for an extended period of time before its pre-emptive maintenance on October 21st, 2014. 56
Figure 19. This figure depicts the mean of all "I" chart values for each DCP accelerator for the ARC. The mean values show that each TrueBeam parameter is distinct across each DCP accelerator. 61
Figure 20. This figure depicts the mean of all "I" chart values for each DCP accelerator for the ATC. The mean values show that each TrueBeam parameter is distinct across each DCP accelerator. 61
Figure 21. This figure depicts the mean of all "I" chart values for each DCP accelerator for the PRC. The mean values show that each TrueBeam parameter is distinct across each DCP accelerator. 62
Figure 22. This figure depicts the mean of all "I" chart values for each DCP accelerator for the PTC. The mean values show that each TrueBeam parameter is distinct across each DCP accelerator. 62
Figure 23. This figure depicts the mean of all "I" chart values at each DCP accelerator for Gantry Speed 2. The mean values show that each TrueBeam parameter is distinct across each DCP accelerator. 63
Figure 24. This figure depicts the mean of all "I" chart values for each DCP accelerator for the Gantry CC Max Values. The mean values show that each TrueBeam parameter is distinct across each DCP accelerator. Most accelerators had similar mean values. 63
Figure 25. This figure depicts the deviations from an overall mean value for each performance parameter in Beam Uniformity Control. The deviations show that each TrueBeam parameter operates at distinct values for each DCP accelerators. 65
Figure 26. This figure depicts the deviations from an overall mean value for each performance parameter in Gantry and MLC Speed Parameters. The deviations show that each TrueBeam parameter operates at distinct values for each DCP accelerators. 66
Figure 27. This figure depicts the deviations from an overall mean value for each performance parameter in Gantry and MLC CC Max Value and LCC Max Value Parameters. The deviations show that each TrueBeam parameter operates at distinct values for each DCP accelerators. 67
Figure 28. This figure depicts the control limits of the "I" chart for each DCP accelerator for ARC. The control limits show that each DCP accelerator has its own operating window. 69
Figure 29. This figure depicts the control limits of the "I" chart for each DCP accelerator for ATC. The control limits show that each DCP accelerator has its own operating window. 70

Figure 30. This figure depicts the control limits of the "I" chart for each DCP accelerator for PRC. The control limits show that each DCP accelerator has its own operating window. 71
Figure 31. This figure depicts the control limits of the "I" chart for each DCP accelerator for PTC. The control limits show that each DCP accelerator has its own operating window. 72
Figure 32. This figure depicts the control limits of the "I" chart for each DCP accelerator for Gantry Speed 2. The control limits show that each DCP accelerator has its own operating window. 73

ABBREVIATIONS

PdM **–** Predictive Maintenance
SPC – Statistical Process Control
GUI – Graphical User Interface
I/MR – Individual/Moving Range
Xbar/R – Average/Range
WFU – Wake Forest University
PMI – Periodic Maintenance Inspections
OEM – Original Equipment Manufacturer
RF – Radio Frequency
A – Amperes
uA – micro amperes
V – Volts
kV – kilovolts
MV – Mega Volts
MeV – Mega Electron Volts
W – Watt
MW – Mega Watts
cm – centimeters
nC – nano Coulombs
HT – High Tension
C – Celsius
SF_6 – Sulfur Hexafluoride
DC – Direct Current
SSD – source-to-skin distance
MLC – Multileaf Collimator
PBC – Process Behavior Charts
UCL – Upper Control Limits
LCL – Lower Control Limits
MC – Morning Check
VMAT – Volumetric Modulated Arc Therapy
IMRT – Intensity Modulated Radiation Therapy
SBRT – Stereotactic Body Radiation Therapy
QA – Quality Assurance
DCP – Data Collection Partnership
CC – Cross-Correlation
2D – two-dimensional
MU – Monitor Units
PFN – Pulse Forming Network
AFC – Automatic Frequency Control

uA – micro Amperes
BRC – Buncher Radial Current
BTC – Buncher Transverse Current
ARC – Angle Radial Current
ATC – Angle Transverse Current
PRC – Position Radial Current
PTC – Position Transverse Current
3D – three-dimensional
LCC – Location of Cross-Correlation
SD – Standard Deviations
PMD – Predictive Maintenance Dashboard
GUIDE – GUI Development Environment
uicontrol – User Interface Control
RGB – Red, Green, Blue
PDF – Printable Document Format
GLCC – Gantry Location of Cross Correlation
PWM – pulse width modulation
ANOVA – Analysis of Variance

ABSTRACT

Modern medical linear accelerators are complex digital devices capable of producing photon and electron beams of multiple energies. These accelerators are comprised of a number of subsystems that facilitate the treatment of cancer using an expanding range of clinical approaches. Accelerator design has interwoven hardware and software such that the opportunity to control components and systems with increasing precision has also increased the ability to monitor system operation. While the manufacturing and design of medical electron accelerators has improved the reliability and consistency of operation, system dysfunction and failure still occur.

Currently, digital data accumulated in the accelerator system are not being exploited in a systematic manner. Linear accelerator interlocks ensure that the operation of the system is discontinued when parameters exceed the limits of a system's operating specifications. Component failure or dysfunction requires immediate repair and service engineering on site. The result is unscheduled machine downtime and disruption of clinical services.

The purpose of this thesis was to develop an effective process for detecting unexpected deviations in accelerator system operating parameters and/or performance that predicts component failure or system dysfunction. The focus of this thesis has three major objectives: (1) Assist in the design of the Statistical Process Control (SPC) database of linear accelerator parameters to detect/predict performance dysfunction; (2) Develop an interface to efficiently display, manage and report the SPC results of all parameters stored in the database; (3) Determine the effectiveness of the standard Individual/Moving Range (I/MR) tests to detect performance dysfunction prior to the actuation of interlocks for several of the parameters under surveillance and the consistency of these parameters being monitored.

I. Introduction

Linear accelerators in radiation therapy are sophisticated machines delivering precise radiation doses to kill cancer cells using digital control systems. Linear accelerators generate digital data that reports the progress of its components during a treatment delivery service. Each component is then monitored internally by the linear accelerator's operating system. Linear accelerator interlocks ensure that the operation of the system is discontinued when parameters exceed the limits of the system's operating specifications [1]. Immediate repair is then required when components fail or dysfunction arises. The result is a disruption of clinical services.

The disruption of clinical services caused by machine downtime can have a number of negative effects. Machine downtime affects scheduled treatment delivery for each patient [2]. Treatment delays can raise the anxiety and stress of the patient. Machine downtime is also not cost-effective, resulting in financial losses to health institutions each year [2]. Properly trained service technicians need to be located and employed as well as replacement components from the manufacturer.

Component failures have the potential to alter the treatment quality and affect delivery of dose to the patient. Alterations to beam quality and dose delivery may result in variable dose to targeted treatment volumes and potentially increase the propensity of damage to critical tissues [2]. The importance of timely maintenance repair and quality assurance cannot be underestimated.

Digital data are not being exploited in a systematic manner to assist in a more efficient deployment of engineering services. Previous work has determined that failure is often preceded by a gradual and measurable deviation of the component's normal operating parameters [2, 3].

Thus, the development of software modules will allow the early detection of these deviations and may allow service engineers to intervene pre-emptively to prevent clinical disruptions.

Currently, a preventive maintenance approach has been taken to maintain proper operation of linear accelerators. Preventive maintenance is defined as "the care and servicing by personnel for the purpose of maintaining equipment and facilities in satisfactory operating condition by providing for systematic inspection, detection, and correction of incipient failures either before they occur or before they develop into major defects" [4]. This type of maintenance includes what is typically known as Periodic Maintenance Inspections (PMI) performed on linear accelerators; the tasks included are the minimum original equipment manufacturer's (OEM) recommended requirements. The basic philosophy behind preventive maintenance is to schedule maintenance activities at periodic time intervals based on calendar days or runtime hours of the machine. The main disadvantage is that scheduled maintenance can result in performing maintenance tasks too early or too late. In addition, there is also the possibility that there could be diminished performance due to incorrect repair methods [5].

In contrast, the philosophy behind predictive maintenance is the idea that repair tasks are performed only when a functional deviation or imminent failure is detected. Using predictive maintenance, mechanical and operational performances are periodically monitored and when unhealthy trends are detected, the troublesome parts are identified and scheduled for maintenance [5]. The physics team at the Wake Forest School of Medicine has put forth the idea of predictive maintenance of medical linear accelerators and formed the Wake Forest Predictive Maintenance (WFU PdM) team.

The overall accelerator predictive maintenance project focuses on the analysis of digital data generated in the TrueBeam accelerator system (Varian Medical Systems, Palo Alto, CA).

This includes the development of software modules to automate the interrogation of treatment performance log files, perform SPC evaluation, and implement a graphical user interface (GUI) for timely review and interpretation of SPC analysis. The focus of this thesis has three major objectives: (1) Assist in the design of the Statistical Process Control (SPC) database of linear accelerator parameters to detect/predict performance dysfunction; (2) Develop an interface to efficiently display, manage and report the SPC results of all parameters stored in the database; (3) Determine the effectiveness of the standard Individual/Moving Range (I/MR) tests to detect performance dysfunction prior to the actuation of interlocks for several of the parameters under surveillance and the consistency of these parameters being monitored.

a. Description of a Linear Accelerator and its Components

Medical electron linear accelerators have continued to evolve since their development in the late 1950's at Stanford University [6, 7]. Modern medical accelerators are complex digital devices producing photon and electron beams at multiple energies. These accelerators are comprised of a number of subsystems that facilitate the treatment of cancer using an expanding range of clinical approaches. Accelerator design has interwoven hardware and software such that the opportunity to control the radiation beam with greater precision has increased [7]. The subsystems that do this, the gantry, the patient support system and the beam defining system, all call for high–quality mechanical engineering [7]. A representation of a medical linear accelerator can be seen in **Figure 1**.

Medical linear accelerators are grouped into five subsystems (1) injection system; (2) Radio Frequency (RF) system; (3) auxiliary systems; (4) beam transport system; and (5) beam collimation and monitoring system [8].

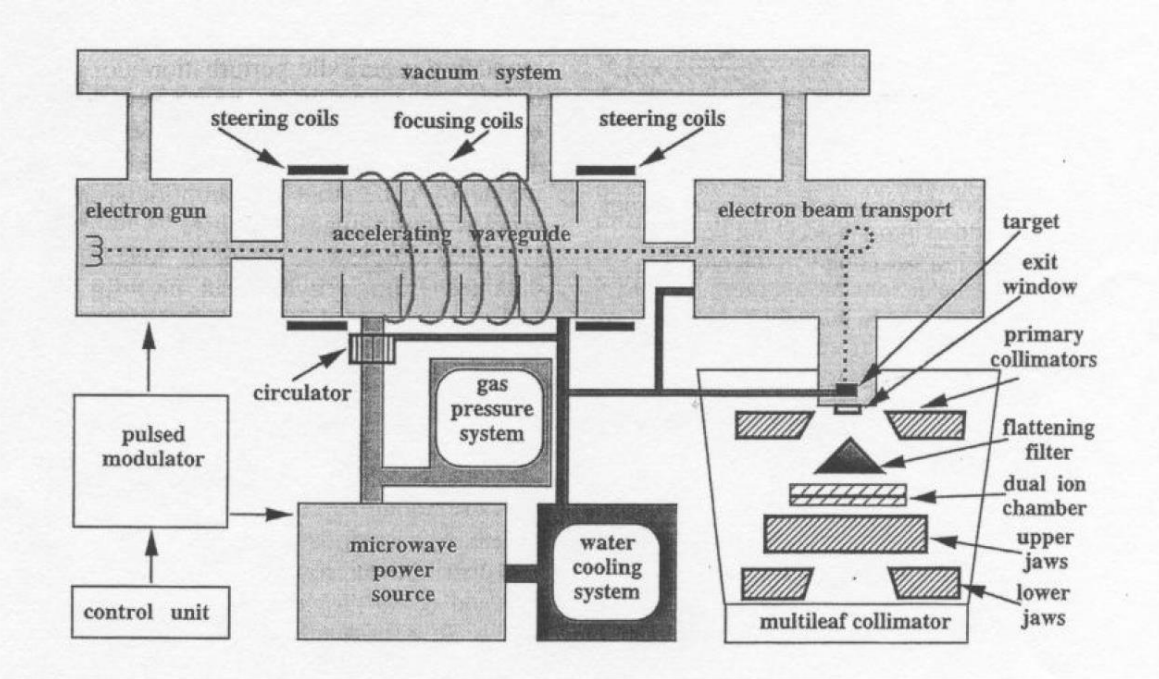

Figure 1. A basic schematic of a medical linear accelerator [8].

The injection system is the source of electrons referred to as an electron gun [8]. An electron gun contains a heated cathode and a grounded anode. Electrons are thermionically emitted from the heated cathode, and accelerated toward the grounded anode, through which they drift to enter the accelerating waveguide. The cathode is heated either directly or indirectly and dependent on the design criteria for electron beam currents to be attained in the accelerating waveguide [6-8]. Voltage pulses control the injection of electrons into the accelerating waveguide and range between -150 V and +180 V [8].

The RF system is used for particle acceleration and consists of several major components: (1) RF power source which is either a magnetron or an RF driver in conjunction with a klystron; (2) a circulator which prevents reverse propagation of RF power from the source to the accelerating waveguide; and (3) accelerating waveguide in which the electrons are accelerated [8].

A magnetron is one of two special types of evacuated electron tubes that is used to provide microwave power to accelerate electrons [6-8]. It is commonly used to power lower energy linear accelerators, typically 12 MeV or less [6]. It is comprised of a cathode, anode, and microwave cavities. Microwave cavities are efficient machined cylinders that allow for high electrical and thermal conductivity [6-8]. Electric current flows along the inner walls and moves electric charges from one cavity end to another. As a result, intense electric fields are produced along the axis of the cavity. Electrons emitted from the cathode are accelerated by a pulsed electric field toward the anode across the evacuated drift space between cathode and anode. Charge distributions (+, -) are then induced on the anode poles and an electric field of microwave frequency is generated between adjacent segments of the anode. Electrons are given a circular arc motion by an imparted magnetic field. As a result, electrons move in complex spirals under these influences [6-8]. This can be seen in **Figure 2.** Approximately 60% of the kinetic energy of the electron beam is converted into microwave energy [6-8]. Microwave energy is then relayed to waveguides.

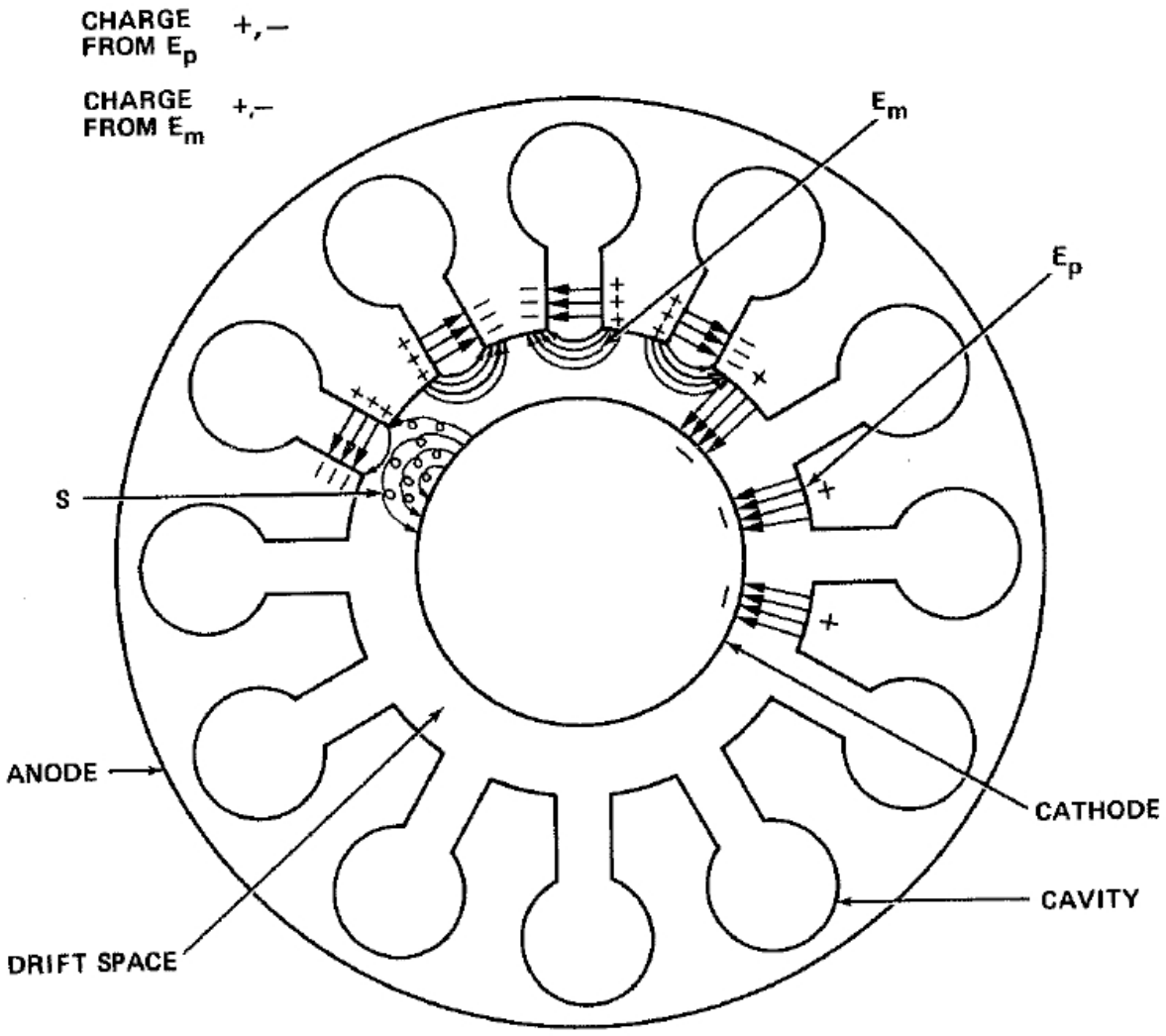

Figure 2. A cross-sectional drawing of a magnetron. E_p represents the pulsed electric field and E_m represents the microwaves. S represents the path the electrons take under the influence of a magnetic field [6].

A klystron is another type of evacuated electron tubes that is used to provide microwave power to accelerate electrons [6-8]. It is generally used in high energy linear accelerators where the production of microwaves with peak power is on the order of 7MW or higher [8]. Electrons are produced at the cathode and accelerated toward grounded cavities. Accelerated electrons pass through two resonant cavities: the buncher cavity and catcher cavity [8]. Electrons passing

through the first cavity are either accelerated or decelerated by the oscillating RF field generated by the RF driver. The "bunched" electrons arrive at the catcher cavity with the same frequency as the resonant frequency of the buncher cavity [8]. If the catcher cavity has the same resonant frequency as the buncher cavity, and is placed with its gap at the bunching position, it will be excited by the electron bunches and the electrons will transfer their energy very efficiently to the RF field of the catcher cavity [8]. This can be seen in **Figure 3**. An RF signal generated by the klystron is then transported to the accelerating waveguide.

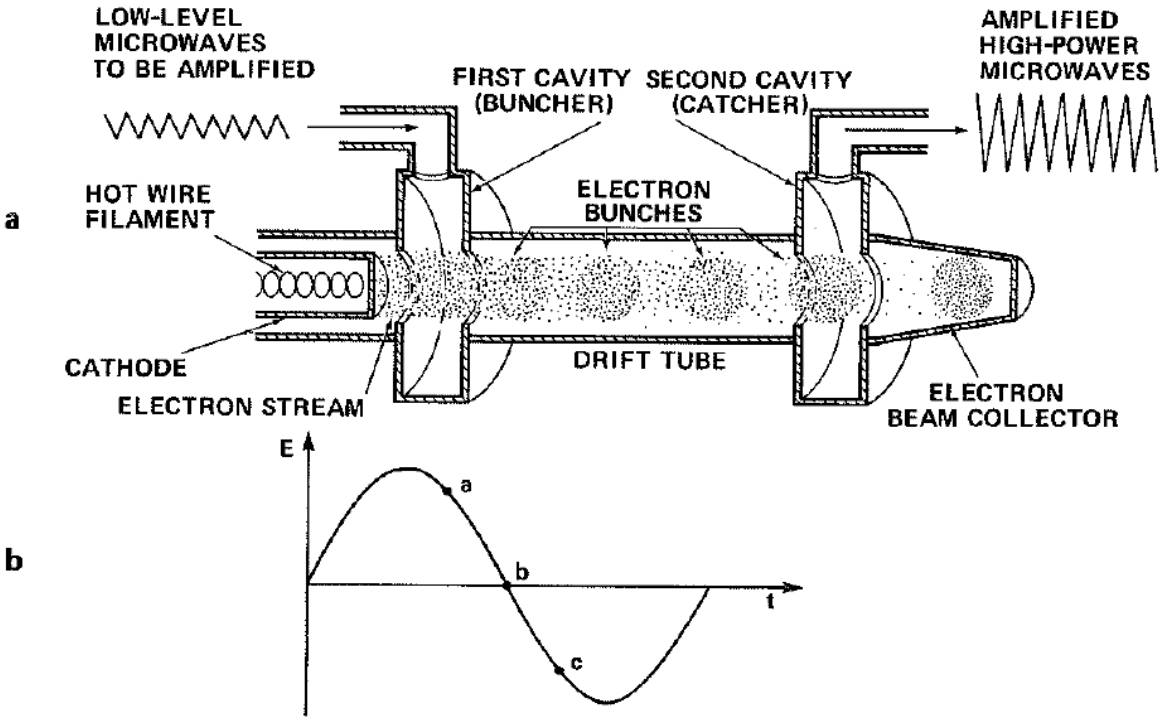

Figure 3. (a) A cross-sectional drawing of a two-cavity klystron tube used as a microwave amplifier. (b) The electric field varies sinusoidally in the first or buncher cavity [6].

Microwave power produced by either the magnetron or klystron is carried to the accelerating waveguide through rectangular uniform S-band waveguides [8]. These waveguides are pressurized with an insulating gas to reduce the possibility of electrical breakdown and thus

increase the power handling capacity. A circulator is also needed to transport microwave power to the accelerating waveguide. A circulator prevents microwave power from reflecting back into the klystron. Reflected microwave power is diverted aside in the circulator, absorbed, and is dissipated through water cooling [6, 8].

An accelerating waveguide comprises the final component of the RF system. Waveguides are evacuated or gas-filled metallic structures of rectangular or circular cross sections used in transferring energy from the electric field to an accelerating electron beam [8]. They vary in length from 30 cm for a 4-MeV unit to more than 1 m for the high-energy units [6]. Cavities accelerate and bunch the electrons like those described in the klystron buncher cavity. They propagate an electric field with increasing velocity in order to further bunch and accelerate the electrons to relativistic velocity. Later cavities provide a constant travelling wave, at the velocity of light. Electrons then gain further energy by increasing their relativistic mass. There are two types of accelerating waveguides: travelling-wave and standing-wave [6].

Travelling-wave accelerator structures consist of a series of hollow cylindrical sections with washer-like disks sandwiched between these sections [6]. Each cylindrical sections and washer-like disks are precisely tuned to a single resonant frequency. This process provides optimal energy gain for the accelerating electrons. Microwave power enters the accelerating structure and propagates towards the high energy end of the waveguide. Accelerating electrons are confined to move up and down the cavity walls while the electric field travels in one direction [6, 8]. This can be seen in **Figure 4a**. Microwave power is then either absorbed without reflection or exits the waveguide to be absorbed or fed back to the input end of the waveguide [6, 8].

In standing-wave accelerator structures, conducting disks are placed at the ends of the accelerating waveguide to reflect microwave power with a $\pi/2$ phase change, resulting in a buildup of standing waves in the waveguide [6, 8]. In this configuration, all even cavities carry no electric field and thus electrons do not gain energy. These cavities serve as coupling cavities and are moved out towards the periphery of the waveguide, effectively shortening the waveguide by 50% [8]. Each cavity only accelerates electrons when the electric field is negative and only in the direction of wave propagation [6-8]. This process continues along the accelerator structure until the electrons acquire their final energy. This can be seen in **Figure 4b**. Unlike travelling-wave accelerator structures, microwave power can be supplied at any convenient location along the accelerating waveguide and preferably directed towards one of the coupling cavities [8].

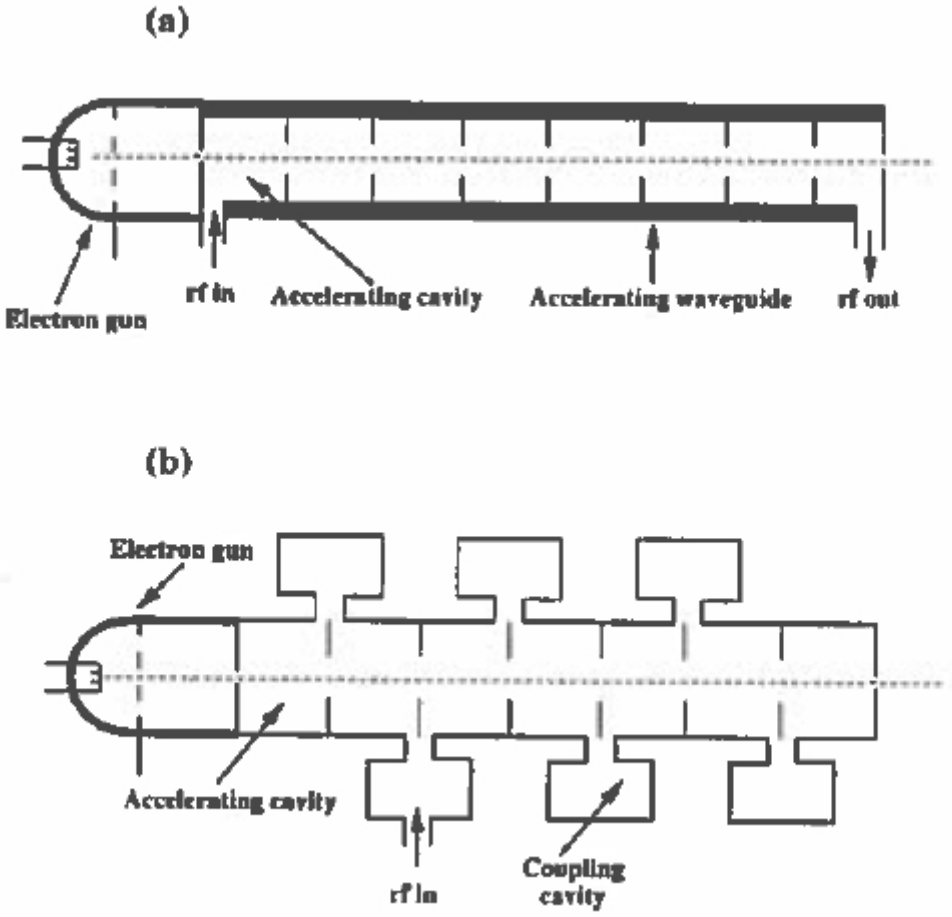

Figure 4. (a) Travelling wave accelerating waveguide. (b) Standing wave accelerating waveguide [8].

The auxiliary system comprises a vacuum pumping system, a water cooling system, a gas dielectric system for the transmission of microwaves from the RF generator to the accelerating waveguide, and shielding against leakage radiation [8]. In order to prevent voltage breakdown, major components of linear accelerators must operate either under a vacuum or at a high gas pressure. Additionally, an evacuated vacuum system prevents scattering of the electron beam in all parts of electron beam transport [7].

The vacuum system is comprised of the transmission waveguide, the electron gun, the accelerating waveguide and the beam transport system [7]. A vacuum system ensures the electrons being accelerated are not deflected by collisions with gas atoms. In other words, the mean free path between collisions with gas atoms needs to be long compared to the length of the accelerating waveguide, the subsequent flight tube [7]. Current technology uses ion pumps to maintain the pressure in the vacuum system. Ion pumps operate as a cold cathode discharge tube. In a cold discharge tube as electrons travel between the cathode and anode, they follow a spiral shaped path that increases the number of electron-gas molecule collisions. As a result, a self-sustaining discharge is achieved at very low pressures [7]. Ion pumps are controlled by a high tension (HT) supply. A control signal proportional to the current can be used within other parts of the accelerator's control circuitry to provide interlocks which will prevent operation of the modulator and the electron gun filament supply if the pressure rises above a pre-determined value [7].

Many parts of the linear accelerator need to be water cooled such as the RF generator, the accelerating waveguide structure, and other parts including beam focusing and steering coils [7]. A water cooling system is used to maintain precise temperature control for stability of operation and prevent overheating and functional failure. Water is supplied at a fixed rate flow and temperature despite the different cooling requirements of each part of the linear accelerator. A reservoir pump circulates water continuously throughout the linear accelerator, preventing components from overheating [7]. Flow control valves and switches allow water to circulate through these components. They also act as interlocks to prevent operation if one of the components is not cooled. The temperature of the water tank in the reservoir is held constant at 1°C by cooling coils. Distilled water is used in these systems because it prevents chemical and

even biological activities which can result in corrosion and/or blockage of pipes and water ways in cooled components [7].

A gas dielectric system is used between the RF generator and the accelerating waveguide. This section needs to be gas filled and operated at high pressures to prevent sparking. It is typically filled with nitrogen, freon or sulfur hexafluoride (SF_6) [7]. A gauge and pressure operated switch, which provide an interlock, inhibits operation if the pressure falls below a pre-set level [7].

Leakage radiation is the bremsstrahlung radiation transmitted through the head of the linear accelerator. Most of the leakage radiation comes from the accelerator target; however, the electron gun, magnetron or klystron, accelerating waveguide, and beam bending magnets may also produce some bremsstrahlung photons in the treatment room. Lead and tungsten shielding is placed around all possible sources of unwanted bremsstrahlung in the linear accelerator [8].

Beam transport system is used to describe how the electron beam is transported from the accelerating waveguide to the exit window for radiation therapy [8]. This is comprised of the steering coils, focusing coils, and bending magnet. Steering coils are used to keep the accelerated electron beam as close as possible to the axis of the cylindrical accelerating waveguide and direct the beam towards the beam transport system. Focusing coils are used to minimize beam divergence and cross section. Stabilized direct current (DC) power supplies produce necessary currents to power the focusing coils [8].

The electron beam leaving the accelerating waveguide and continues through an evacuated bending magnet system [6]. The bending magnet deflects the electron beam to either strike a target for photon therapy or to exit through a thin metallic window for electron therapy.

Table I describes the three systems for beam bending that have been developed: (1) 90° bending; (2) 270° bending; and (3) 112.5° bending [6].

Table I: **Bending Magnet Systems**	
Bending	**Description**
90° bending	Higher energy electrons in the electron beam spectrum are bent less than lower energy electrons; Defocuses and spreads the electron beam,
270° bending	Achromatic; Refocuses electron beam spread and directional spread; provides small focal spot on x-ray target;
112.5° bending	Achromatic; Requires no more vertical space than 90° bending,

The treatment head contains components necessary for beam collimation and monitoring systems [6, 8]. Different components within the treatment head can been in **Figure 5**. These systems provide the shaping, manipulating, and monitoring of the clinical x-ray or electron beam. A flattening filter, a conical metal absorber, absorbs photons from the central axis of the beam to provide uniform x-ray treatment fields. A scattering filter is used in electron beam therapy and spreads out the pencil-like beam to provide uniform electron treatment fields. A carousel facilitates the exchange between the differing filters. Other devices contained in the treatment head include the field defining light which simulates the x-ray field. The area to be irradiated is illuminated on the patient's skin surface and facilitates positioning the patient for x-

ray treatment. A range finder light projects a numerical scale on the patient's skin to indicate the source-to-skin distance (SSD) typically from 80 to 130 cm on the central axis [6, 8].

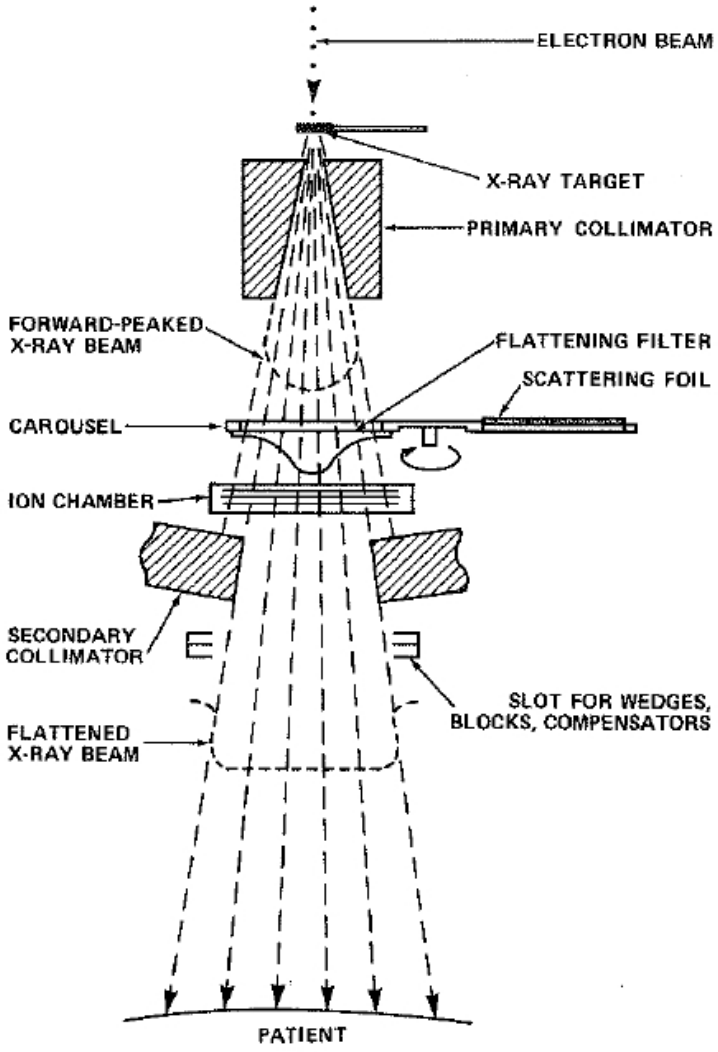

Figure 5. Auxiliary components of a medical linear accelerator system [6].

Beam collimation is achieved with two or three collimator devices for photon beams: (1) primary collimator; (2) second movable beam-defining collimators; and (3) multileaf collimator [6, 8]. Clinical electron beams also rely on electron beam applicators for beam collimation [6, 8]. The primary collimator limits the maximum field size for x-ray therapy. It is a conical opening machined into a tungsten shielding block with the sides of the conical opening projecting onto

edges of the target on one end of the block and onto the flattening filter on the other end. The thickness of the shielding block is usually designed to attenuate the primary x-ray beam intensity to less than 0.1% of the initial value [8].

The second movable beam-defining collimators consist of four thick metal blocks, called jaws, often made of tungsten which helps provide sharp edges for treatment fields [6]. Two blocks form the upper jaws and the remaining two form the lower jaws of the collimator. Jaws provide symmetric and asymmetric fields depending on the design of the linear accelerator [8]. The movement of the jaws is confined to arcs so that the block faces present a flat edge to the beam diverging from the target [6].

The multileaf collimator (MLC) consists of a pair of jaws that are divided into small computer controlled leaves that may range from 60 to 160 depending on MLC design [6, 8]. Leaves can be arranged accordingly to adapt to individual patient tumor size and shape. By using multiple fields with MLCs, the tumor dose in comparison to standard techniques can be increased while additional normal tissue is spared by tightly conforming the treatment fields to the tumor volume. Dynamically controlling MLC motion permits the modulation of the intensity within a photon beam. This added degree of freedom further allows for better conformity.

Linear accelerators are equipped with dose monitors to monitor the beam output continuously during patient treatment [8]. Two transmission ionization chambers are permanently imbedded in linear accelerators and are placed between the flattening filter or scattering foil and the photon beam secondary collimator. The main requirements for the ionization chamber are: (1) the chambers must have a minimal effect on radiation beams; (2) their response should be independent of ambient temperature and pressure; and (3) they should

be operated under saturation conditions [8]. The beam monitoring system also monitors the beam energy, beam flatness and symmetry as well as the dose rate [8].

For patient safety, each ionization chamber has completely independent biasing power supplies and readout electrometers. If the primary chamber fails during patient treatment, the secondary chamber will terminate the irradiation. In the event of a simultaneous failure of both ionization chambers, the linear accelerator timer will shut the machine down with minimal overdose to the patient [8].

b. System Interlocks

Normal operation of components and parameters within the linear accelerator are controlled by machine controls and interlocks, treatment controls and safety interlocks [7]. Interlocks ensure that the accelerator will operate only if the correct conditions are satisfied. This requires correct preparation, correct selection of machine settings and then proper operation of the machine [7]. Machine controls and interlocks are used to ensure that the accelerating waveguide and its associated components operate according to specification and that it is energized only when it is safe to do so; they are there to protect the machine itself [7]. Safety interlocks are used to protect the patient and staff from the many dangers that arise in the operation of these machines such as mechanical and electrical changes [7]. Lastly, treatment controls and interlocks are used to set up the accelerator to treat each individual patient and to ensure that the radiation output is consistent with the treatment prescription [7]. The overall interlock system helps to prevent serious injury to patients and staff and major damages to the machine.

c. Current Maintenance Procedures and the Impact of System Downtime

Current maintenance procedures for medical linear accelerators fall into two distinct categories: PMIs and Service Calls. The PMI is essentially the manufacturer's preventive maintenance program consisting of one or more scheduled maintenance inspections per year. Typically, a checklist is provided to service personnel that indicates the frequency and targeted tasks for each PMI; this would include quarterly, semiannual, and annual tasks. These tasks run the full gambit from simply replacement of labels and log sheets to ensuring beam quality and adherence to all patient safety concerns. Some of these tasks may be performed during or subsequent to routine service calls. Routine service calls, however, involve a specific investigation based on performance issues reported by the facilities and/or operator. During these calls, the service representative is focused on troubleshooting system or component malfunction. It is evident when reviewing this type of maintenance system that effort is expended in reviewing and servicing systems that may not need servicing; More critical systems may in fact not be serviced at the proper frequency.

Complex systems such as linear accelerators require specific maintenance procedures to ensure optimal performance that results in high quality care for patients. Poor maintenance procedures can cause disruption within the clinic such as machine downtime. Patients then have to wait longer while technicians and in-house staff try to diagnose and repair the issue [9]. Additional costs and rescheduled treatment appointments are then enacted, raising the stress of the patient as well as on their family. A predictive maintenance system would alleviate these disruptions and allow for stable work flow in radiation therapy.

II. Statistical Process Control and Its Uses

a. General Information

SPC is an analytical measure of normal and abnormal variation of a process [10, 11]. SPC is used globally in manufacturing and business management to provide an ongoing evaluation of the stability and/or variability of a specific component [10, 11]. Its success rests upon the fact that any process can be mapped by a series of inputs and outputs. SPCs are displayed using process behavior charts (PBCs) which are graphs that contain data from a chosen process and can detect the stability of the chosen process [10-12]. Action limits are calculated from the chosen process and aid in determining its stability and predictability. A process is predictable when it is in a state of statistical control, and it is unpredictable when it is not in a state of statistical control [10-13]. SPC facilitates the characterization and control of a process using probability and statistics as a data driven graphical tool.

b. Techniques: Xbar/R and I/MR Charts

A PBC is a graphical display that contains the following elements: groups of data points that represent different values at different times during a specified process, the mean of the data points - a center line that is drawn at the mean value of the data points, upper and lower control limits that indicate the threshold at which the process output is considered statistically “unlikely” and are drawn typically at 3 standard errors from the center line [10-13]. PBCs allow for rapid and simple detection of events that are indicative of actual process change. When change is detected and considered necessary, action can readily be taken and become the new way of working. In contrast, when the change is bad and considered detrimental, action can readily be identified and eliminated. PBCs help draw conclusions about whether the process variation is consistent or unpredictable [10-13].

PBC consists of two distinct charts: Xbar (average) and R (range) charts that is used to monitor data points when samples are collected by regular intervals from a process [10-13]. Xbar/R charts are advantageous when a particular process can be monitored in both the location and the dispersion of the values. At a given point in time, several measurements will be obtained, and these values will then be grouped together and treated as a separate set of data. These charts plot the mean value for the process across all measurements in the sample plus the range of the process across all measurements in the sample [10-13]. This can be seen in **Figure 6**. If the process is stable and constant, Xbar/R charts will show the measurements moving in a random behavior. The PBC's purpose is to detect nonrandom behavior of a process or parameter.

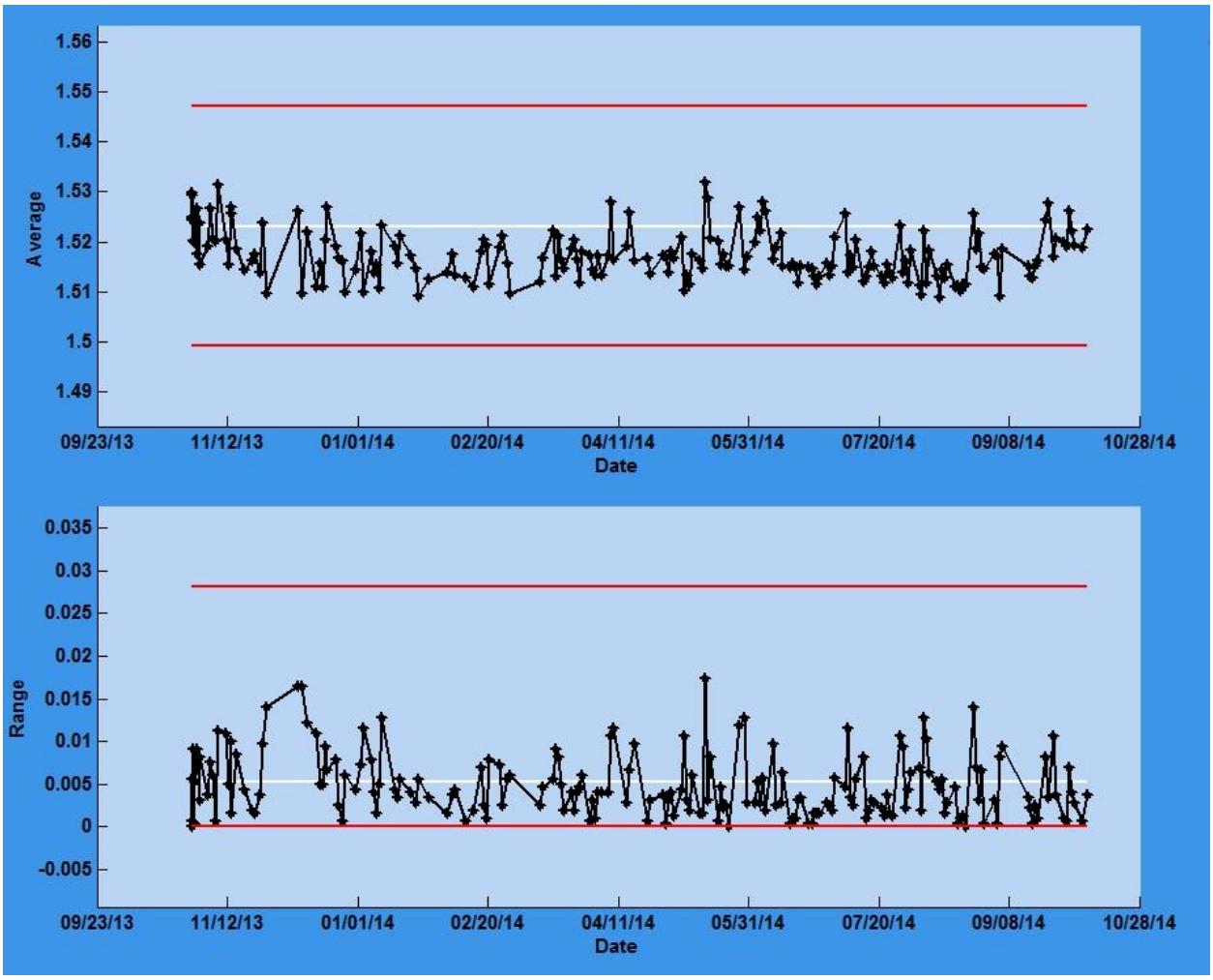

Figure 6. A basic schematic of an Xbar/R chart.

Xbar/R chart values are calculated using the following schematic: given *k* subgroups, where each subgroup consists of *n* observations:

$$\bar{X}_k = \frac{\sum(X_n)_{n=1\ldots n}}{n} \tag{1}$$

$$R_k = R_n - R_{n-1} \tag{2}$$

$$\bar{\bar{X}} = \frac{\sum(X_k)_{k=1\ldots k}}{k} \tag{3}$$

$$\bar{R} = \frac{\sum(R_k)_{k=1\ldots k}}{k} \tag{4}$$

The central line for Xbar chart is the Grand Average, $\bar{\bar{X}}$, and the central line for R chart is the Average Range, $\bar{R}$. d_2 and d_3 are constants that reflect the non-normality of the distribution of range values and depend on *n*. An asymmetric distribution is seen by the range limits about the mean range because the range is a positively skewed value. [10-12, 19-20]. The limits, upper control limit (UCL) and lower control limit (LCL), are then calculated.

$$UCL_{\bar{X}} = \bar{\bar{X}} + 3\frac{\bar{R}}{d_2\sqrt{n}} \tag{5}$$

$$LCL_{\bar{X}} = \bar{\bar{X}} - 3\frac{\bar{R}}{d_2\sqrt{n}} \tag{6}$$

$$UCL_R = (1 + 3\frac{d_3}{d_2})\bar{R} \tag{7}$$

$$LCL_R = (1 - 3\frac{d_3}{d_2})\bar{R} \tag{8}$$

I/MR chart is another type of PBC that is used to monitor a process as independent observations. The division of a process into sub-processes increases the efficacy of detecting system changes or inappropriate variations within that process. This PBC consists of a pair of charts: (1) an individual chart which displays the individual measured values and (2) a moving range chart which displays the difference from one point to the next. Unlike measurements in Xbar/R charts being grouped together as a single instance in time, measurements in I/MR charts are treated as independent observations for all instances in time [10-13]. Control limits are also utilized because they can correctly describe the predictive role these limits play when the data display a reasonable degree of statistical control. Control limits are calculated based on the variation of the measurements rather than chart limits that are pre-defined to control predictability. This can be seen in **Figure 7**.

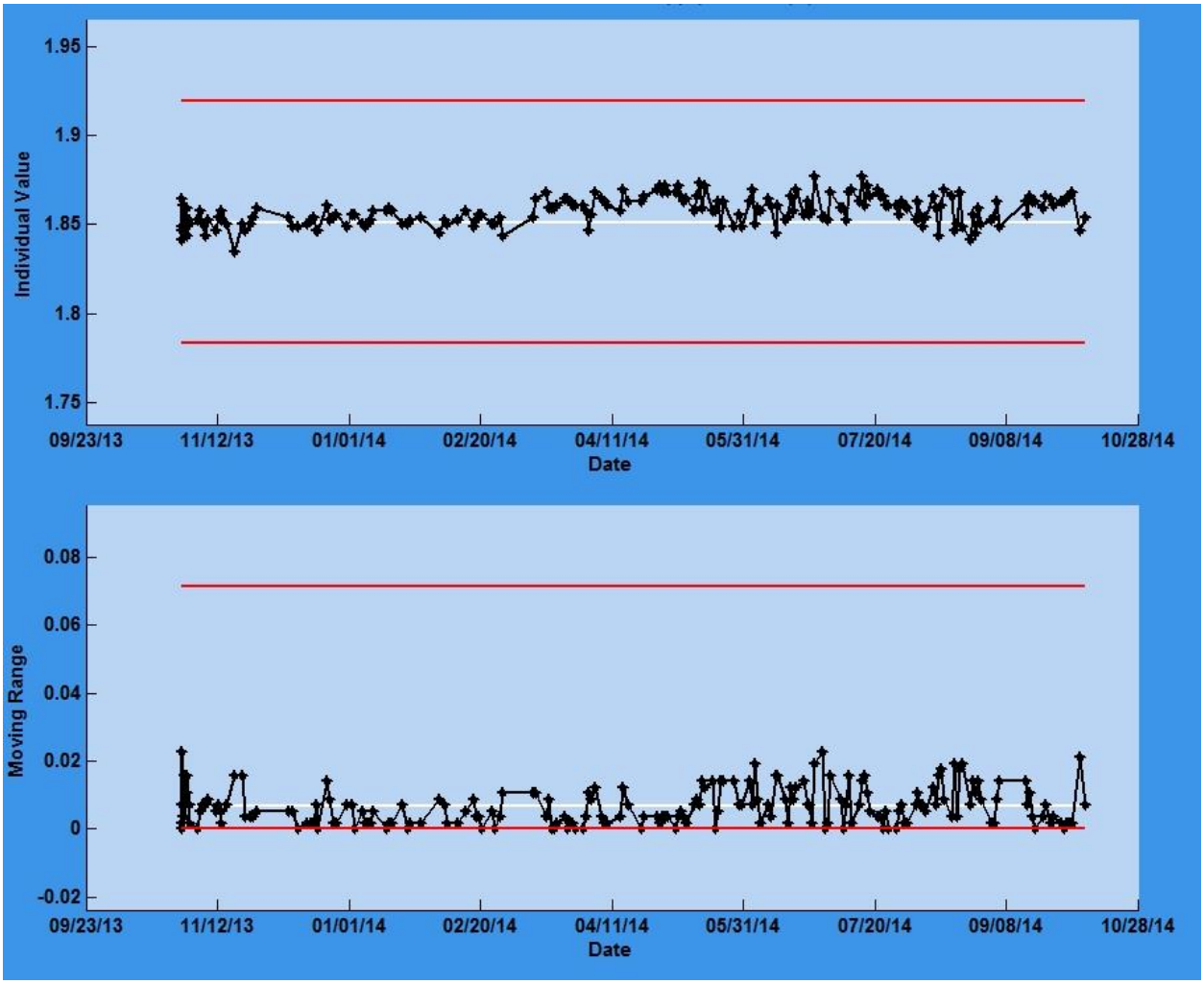

Figure 7. A basic schematic of an I/MR chart.

I/MR statistical values are calculated using a similar schematic in Xbar/R charts; however, chart control limits are calculated using the following schematic:

$$\bar{I} = \frac{\sum(I_n)_{n=1\ldots.n}}{n} \tag{9}$$

$$MR = |x_n - x_{n-1}| \tag{10}$$

$$\overline{MR} = \frac{\sum(MR_n)_{n=1\ldots.n-1}}{(n-1)} \tag{11}$$

The central line for the Individual Value chart is the Grand Mean, $\bar{I}$, and the central line for the Moving Range chart is the Average Moving Range, $\overline{MR}$.

$$UCL_I = \bar{I} + \frac{3\overline{MR}}{d_2} \tag{11}$$

$$LCL_I = \bar{I} - \frac{3\overline{MR}}{d_2} \tag{12}$$

$$UCL_{MR} = (1 + 3\frac{d_3}{d_2})\overline{MR} \tag{13}$$

$$LCL_{MR} = (1 - 3\frac{d_3}{d_2})\overline{MR} = 0 \tag{14}$$

c. Previous work of the use of SPC on Linear Accelerators

SPC has shown promise as a reliable analytical tool in radiation oncology. Processes in this field have numerous nonrandom and systematic errors that are not easily detected using quality assurance practices; these errors consist of mainly small random errors and a very few number of large errors. SPC allows the differentiation between these errors and the ability to detect the dominant source(s). SPC has been used in notable processes in radiation therapy such as beam steering, dosimetric performance, and most importantly, quality assurance of linear accelerators to note and eliminate erratic behavior [1-3, 14-18].

SPC used in accelerator performance and reliability

In radiation therapy treatment, high energy x-ray beams must exhibit uniformity; uniformity is based in terms of flatness and symmetry. The electron beam must be accurately delivered onto the x-ray target so that the focal spot is aligned with the beam flattening filter. Also, electrons must be accelerated to the correct energy because the flattening filter shape is specifically tailored to a particular energy. Beam uniformity is achieved by steering the beam to a specific location (position) and exit orientation (angle) as it strikes the target. Two sets of steering coils are used to direct the beam onto the target. The first set of coils is found on the

solenoid of the waveguide and the second set of coils is in the electron beam transport section prior to the beam striking the target.

Linear accelerators analyze beam uniformity internally by using ion chambers located below the flattening filter. The beam current measured in each quadrant is compared and any asymmetry exceeding the specification results in a system interlock. Our group at the Wake Forest School of Medicine sought to characterize the process of medical linear accelerator beam steering and demonstrate, retrospectively, the ability to provide a level of control using SPC. They believed that SPC could ensure consistency of beam uniformity and indicate when intervention is required to correct non-uniformity prior to the actuation of a system interlock. They acquired data from a Varian 21EX that experienced downtime due to an unreported issue related to a water leak in the gantry stand; the leak affected the beam symmetry by 2%. The machine was eventually repaired and all beams were scanned and adjusted to ensure beam flatness, symmetry, and absolute dose outputs were within operating specifications. Data from September 2009 until two weeks following the beam steering failure in June 2010 were evaluated. Using morning warm-up measurements at a single standard gantry angle, they extracted the steering coil current values (amperes) for the transverse and radial plane position and angle steering coil current values from generated morning check (MC) files. Processes were monitored using Xbar/R charts.

The results of this study suggested that SPC analysis would have provided an early indication of deviations in the current values prior to the actuation of the interlock and unscheduled downtime. SPC analysis of the transverse angle of steering coil currents showed a downward trend until failure; transverse position steering coil currents showed a similar trend. Analysis of the steering coil currents in the radial plane did not show a similar trend as early as

the steering coil current in the transverse plane. SPC charts confirmed that the water leak and resulting damage persisted for a relatively long period of time. Simply using data points exceeding chart limits as a service intervention would have resulted in repair of the leak prior to the actuation of the system interlock. In summary, the use of an SPC subsystem in medical linear accelerators can monitor consistency of operation, ensuring consistent operating parameters relative to the baseline values determined at the time of accelerator commissioning.

III. Predictive Maintenance Model for Medical Linear Accelerators

The physics team at the Wake Forest School of Medicine has put forth the idea of predictive maintenance of medical linear accelerators and formed the WFU PdM team. The predictive maintenance model rests upon the theory of detecting unexpected deviations in accelerator system operating parameters and/or performance. In turn, maintenance can be performed prior to the actuation of interlocks. Performance characteristics critical to the delivery of high quality dynamic treatment (Volume Modulated Arc Therapy (VMAT), Intensity Modulated Radiation Therapy (IMRT), Stereotactic Body Radiation Therapy (SBRT), and Gated delivery) are: (a) gantry speed and position fidelity, (b) MLC leaf speed and position fidelity as a function of gantry position, and (c) beam uniformity (steering) as a function of gantry position. Accelerator systems under optimal circumstances operate with random variation that can be modeled by a continuous probability density function. By establishing the mean operating values using SPC methodology and continuously sampling these values, detection of unexpected deviations that predict component failure or system dysfunction becomes possible [10-12, 19-21]. The use of performance data within a systematic, integrated SPC framework can be deployed as a PdM program for medical linear accelerators.

The proposed PdM approach is as follows: 1) deliver a daily quality assurance (QA) treatment; 2) automatically transfer and interrogate the resulting log files; 3) once baselines are established, subject daily operating and performance values to SPC analysis; 4) determine if any alarms have been triggered; and 5) alert facility and system service engineers. Software modules will be developed to automate the interrogation of treatment performance log files, perform the SPC evaluation, and display the results in a graphical dashboard interface.

A data collection partnership (DCP) of five facilities has been formed monitoring seven digital accelerators. Partners are asked to deliver a robust VMAT treatment each day [22]. The log files resulting from the treatment are transferred, decoded, analyzed, regrouped and subjected to SPC analysis. The field service reports for each accelerator are submitted and tracked in tandem with the SPC analysis. The project has been conducted in the run-to-failure format, meaning that no active service intervention is initiated solely as a result of data analysis. Each facility has maintained autonomy in determining when and what level of accelerator maintenance will be performed.

a. Daily QA Treatment Delivery and File Transfer

A daily VMAT QA treatment delivery (Snooker Cue) is utilized to assess the interplay between gantry angle, MLC position and dose delivery in a single treatment [22]. Characteristics of Snooker Cue delivery that are of particular interest are the dose delivery at narrow angular sectors that provides maximal gantry acceleration and deceleration, and the delayed displacement of the MLC gap from one position to the other which enforces maximum leaf speed before coming to an abrupt halt at the moment of delivery. The four subarc fields characteristic of Snooker Cue tests were integrated into a single delivery using the automated delivery feature of the accelerator. Treatment performance logs are written for each treatment delivery and are accumulated on the accelerator server.

Each DCP facility is provided a cloud storage account and the ability to sync a local folder. Automated daily log file transfer allows for daily analysis and review.

b. File Decoding, Data Analysis and Regrouping

All computer code is written in MATLAB [23]. Treatment performance logs consist of trajectory and text log files which are decoded by separate functions. The text log is written at

the start of the delivery and contains a single snapshot of 45 data values. There is no processing of these data. The trajectory logs contain parameter data taken every 20 msec during the delivery. Each trajectory file is decoded and a total of 131 axis positions are chosen to be recorded (collimator jaw position, gantry angle, each MLC, etc). These raw data are processed and axis positions are extracted at critical points during the delivery. Where axis velocity is evaluated, it is determined by positional change over time. The focus of our analysis is the accuracy, reproducibility and fidelity of each axis. A reference positional trace of the gantry and each MLC is used as a motion baseline for cross-correlation (CC) analysis. The trajectory logs of 495 parameters are analyzed, 482 of which are MLC related. A total of 525 operational or performance parameters are monitored (35 text log and 490 trajectory log) using SPC analysis.

c. SPC Analytical Formulism and Evaluation Guidelines

In this project the use of I/MR charts is the chosen SPC approach since each value is identified with a specific period of time - daily. Since it is impractical to deliver the QA treatment multiple times each day, the logical subgroup size for single daily delivery is n=1. While I/MR charts are the most sensitive in identifying changes in parameters, our methods for calculating the chart limits and chart analysis rules will determine how effective we can predict when maintenance intervention is necessary. The experience of the WFU PdM team has shown that the use of traditional SPC chart limits (±3 standard deviation (±3 σ) from the grand mean) can result in an unacceptable rate of false positive signals [24, 25]. Using information on system specifications from the manufacturer, consulting the literature for recent studies on quality control of complex treatment delivery (IMRT, VMAT, SBRT, etc) and white papers on quality assurance of linear accelerators, the WFU PdM team introduced a hybrid approach to calculating

the control chart limits that includes a factor (S_p) that fractionally increases the limits based on the operational parameter specification and/or performance criteria ($\pm 3\ \sigma_{hybrid}$) [26-29].

Individual grand mean, moving range and grand mean (I/MR) chart values are determined as follows:

$$\bar{I} = \frac{[\sum I_{t_{t=1\ldots T}}]}{T} \tag{14}$$

$$MR_t = |I_t - I_{t+1}| \tag{15}$$

$$\overline{MR} = [(\sum MR_t)_{t=1\ldots T-1}]/(T-1) \tag{16}$$

where T = 20 (for initial use but the value of T may be altered at a later date by the user via the dashboard interface) and I_t is the individual value of the component. Control limits are then calculated.

For individual upper and lower control limits:

$$3_{\sigma(\bar{I})hybrid} = \left[\left(\frac{3}{d_2}\overline{MR}\right) + S_p\right] \tag{17}$$

$$UCL_I = \bar{I} + \left[\left(\frac{3}{d_2}\overline{MR}\right) + S_p\right] \tag{18}$$

$$LCL_I = \bar{I} - \left[\left(\frac{3}{d_2}\overline{MR}\right) + S_p\right] \tag{19}$$

For moving range control limits:

$$3_{\sigma(\overline{MR})hybrid} = \left[\left((1 + 3\frac{d_3}{d_2})\overline{MR}\right) + S_p\right] \tag{20}$$

$$UCL_{MR} = \left[(1 + 3\frac{d_3}{d_2})\overline{MR}\right] + S_p \tag{21}$$

$$LCL_{MR} = \left[(1 - 3\frac{d_3}{d_2})\overline{MR}\right] + S_p = 0 \tag{22}$$

This hybrid approach increases the variance and kurtosis of the parameter probability density function. This is illustrated for transverse beam symmetry in **Figure 8**.

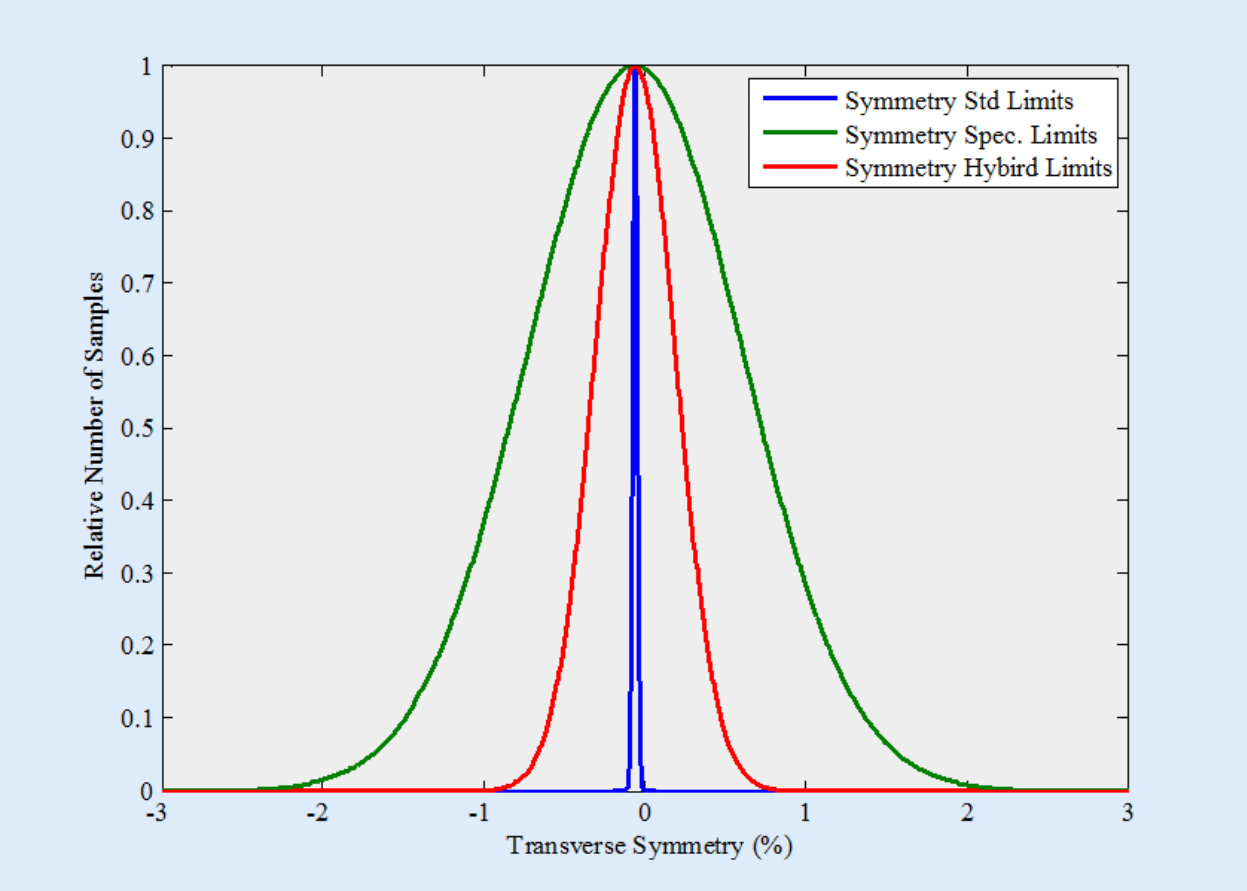

Figure 8. Normal probability density functions representing three "I" chart limit calculation methods for 6 MV photon transverse symmetry: traditional/standard SPC, symmetry specification (±2%), and our hybrid method that includes the standard SPC calculation and an empirical factor (S_p).

Individual chart warnings and alarms are determined by:

a. Alarms: 2 of 3 or 3 of 5 consecutive data points exceeding the upper or lower control limits ($\geq \pm 3\sigma_{(I)hybrid}$);

b. Warnings: 2 of 3 or 3 of 5 consecutive data points exceeding $\pm 2\ \sigma_{(I)hybrid}$ from the grand mean.

Moving Range chart warnings and alarms are determined by:

a. Alarms: 3 of 5 consecutive data points exceeding the upper control limit ($\geq 3\sigma_{(R)hybrid}$);

b. Warnings: 3 of 5 consecutive data points exceeding +2 $\sigma_{(R)hybrid}$ from the mean.

d. Database Design

A SPC data repository consisting of a multidimensional matrix is created for each accelerator along with several reference files specific to its baseline performance. This data repository combines both text and trajectory log files into a single matrix that allow for rapid interrogation via a GUI. Text files contain 45 system parameters pertaining to one of the following categories: RF generation, electron gun control, energy control, beam uniformity control, DC voltage generation, and cooling systems. The remaining system parameters (490) are contained in trajectory log files and pertain to collimator jaw positions, MLC carriages, gantry angle, and MLC leaves. Engineers and physicists view the results in I/MR charts.

<u>New Machine Setup</u>

The following data files are needed.

Gan (two-dimensional (2D) matrix) – cross-correlation baseline for Gantry

corr_mlc (2D matrix) – cross-correlation baseline for all MLC

1. The path of the data files is determined and used to decode each pair of .bin and .txt files

2. The (1) datenumber of the delivery is determined from the filename.

3. There is no processing of the textdata. There are 45 data values determined from the .txt file; it is a single row with 45 columns consisting of the following data (in order):

2) X1

3) X2

4) Y1

5) Y2

6) Gantry Angle (deg)

7) Monitor Units 1 (MU1)

8) Monitor Units 2 (MU2)

9) Radiation Time (mins)

10) DoseRate (MU/min)

11) Pulse Forming Network (PFN) High Voltage Power Supply Current (A)

12) PFN Actual Voltage (KV)

13) RF Driver Voltage (V)

14) RF Forward Power (W)

15) Automatic Frequency Control (AFC) Error (V)

16) Gun Current (A)

17) Gun High Voltage (V)

18) Gun Grid Voltage (V)

19) Gun Filament Step Voltage (V)

20) Gun Filament Voltage (V)

21) Bend Magnet Current (A)

22) Bend Magnet Voltage (V)

23) Accelerator Solenoid Current (A)

24) Klystron Solenoid Current (A)

25) Radial Symmetry (%)

26) Transverse Symmetry (%)

27) Target Current (nC)

28) Buncher Radial Current (BRC) (A)

29) Buncher Transverse Current (BTC) (A)

30) Angle Radial Current (ARC) (A)

31) Angle Transverse Current (ATC) (A)

32) Position Radial Current (PRC) (A)

33) Position Transverse Current (PTC) (A)

34) Trim: (A)

35) Accelerator Vacion Current (uA)

36) Positive 5V dc

37) Positive 24V dc

38) Analog Negative 5V dc

39) Analog Positive 5V dc

40) Negative 12V dc

41) Positive 3V dc

42) Node Power Supply Voltage (V)

43) Water Level

44) City Water Temperature (°C)

45) Internal Water Supply Temperature (°C)

46) Gas Pressure (psi)

5. The trajectory data is a 2D matrix with the dimensions (20msec snapshots (rows) x 131). The 131 columns consist of the following data (in order):

Y1

Y2

X1

X2

Couch Vertical

Couch Longitudinal

Couch Lateral

Couch Angle

Carriage A

Carriage B

Gantry Angle

MLC Bank A (60 leaves) – leaf position

MLC Bank B (60 leaves) – leaf position

This matrix is processed to extract values at predetermined location(s) that are specific to the QA VMAT delivery (Snooker Cue) developed by Van Esch et al.

6. The trajectory data is processed and results in a single row of 494 values. The 494 columns consist of the following data:

47) Y1

48) Y2

49) X1

50) X2

51) Couch Vertical

52) Couch Longitudinal

53) Couch Lateral

54) Couch Angle

55) Carriage A

56) Carriage B

57 & 58) Gantry – Speed 1, Speed 2

59 – 178) MLC Bank A (60 leaves) – each leaf: Speed 1, Speed 2

179 – 298) MLC Bank B (60 leaves) – each leaf: Speed 1, Speed 2

299 & 300) Gantry – cross-correlation max value, location of cross-correlation (LCC) max value

301 – 420) MLC Bank A (60 leaves) – each leaf: cross-correlation max value, location of cross-correlation max value

421 – 540) MLC Bank B (60 leaves) – each leaf: cross-correlation max value, location of cross-correlation max value

7. The row values are concatenated into a vector.

8. All files processed during this initial session are accumulated into a matrix named 'dataout'

9. Each column of 'dataout' is treated as an independent parameter for SPC analysis.

10. 'SPC_NewMachine' is a three-dimensional (3D) matrix (#rows, 540, 19). Each row of data corresponds to a single delivery of the RapidArc QA treatment. The 19 2D matrices are as follows:

1) Raw Data

2) Individual

3) MR value

4) Grand Mean – Individual (first 20 samples)

5) Grand Mean – MR (first 20 samples)

6) Upper Control Limit – Individual

7) Lower Control Limit – Individual

8) Upper Control Limit – MR

9) Lower Control Limit – MR

10) Limits Exceeded – Individual

11) Limits Exceeded – MR

12) 2 Standard Deviations (SD) Exceeded – Individual

13) 2SD Exceeded – MR

14) Warning – Individual

15) Warning – MR

16) Alarms – Individual

17) Alarms – MR

18) Stage – counts number of stages of analysis based on updates to "I" chart limits

19) Flag – counts number of data points within each Stage

IV. Interface Development and Use

The development of a dashboard interface to display and evaluate the results of the SPC charts is an integral part of this project. The dashboard is modeled after traditional SPC charts used in manufacturing that include the control chart, a horizontal frequency distribution of data samples, statistical summary of control chart parameters and other data, as well as insertion and display of user comments for each parameter [11]. Additional features include parameter status recognition and representation, user determined chart limit revisions, zoom in/out, and report generation. The MATLAB programming environment (Mathworks, Natick, MA) was used to develop the predictive maintenance dashboard (PMD) [23].

MATLAB enables the creation of GUIs which is a graphical display in one or more windows containing user-operated controls or components. The user of the GUI does not have to create a script or type commands at the command line to accomplish tasks. GUIs wait for a user to manipulate a control, and then respond to the user action. Each component in the GUI has one or more callbacks which are actions that call MATLAB to perform a specific task. A particular user action, such as pressing a screen button, triggers the execution of the callback, in which the GUI responds to the action. Components such as menus, toolbars, push buttons, radio buttons, list boxes, and sliders can be built and programmed into the GUI to perform interactive tasks. They can also perform computations, read and write data files, communicate with other GUIs, and display data as tables or plots. A GUI can be built by two means: (1) GUI Development Environment (GUIDE) which is an interactive GUI construction kit or (2) Programmatic GUI Construction which are user-generated code files that generate GUIs as functions or scripts. In this project, the PMD was built by programmatic construction.

MATLAB GUIs built using programmatic construction allows the creation of complex GUIs that require advanced needs and functionality beyond the limited scope of GUIDE [23]. Often times, GUIs created from programming are used to interact with other GUIs. The GUI developed in this work needed precise control and placement of all of its components and behaviors. The process provided by programmatic GUI allows for an easy production of an interface using code files that define all component properties and behaviors. When a user executes the file, it creates a figure, populates it with components, and handles user interactions.

GUI components perform a specific task and have a well-defined set of properties. There are a number of GUI components available; however, this project utilizes three in particular: figure, axes, and uicontrol. **Table II** describes each GUI component.

Table II: MATLAB GUI Components

Functions	**Description**
Figure	Create figure window
Axes	Create axes graphics object
uicontrol	Create user interface object

Figure window provides a framework for the other controls. It serves to effectively present the GUI components and provides an overview of the task to be accomplished in them. The most common properties used to define the various figure windows in the PMD are presented in the **Table III**.

Table III: MATLAB Figure Properties

Property	**Description**
Color	Sets the figure window background color

MenuBar	Turns system-level menus on/off
Name	Sets the figure window title
Position	Sets location and size of figure's drawable area
Resize	Sets window resize mode on/off
ToolBar	Sets figure toolbar display on/off
Units	Defines the units of measurement

The 'Color' property is often described by RGB (red, green, blue) color triples; [1 1 1] represents white, [0 0 0] represents black, and [1 0 0] represents red. Each of the three numbers can be any decimal value from 0 to 1 such that different combinations yield colors outside the MATLAB standard. The 'Position' property is measured from the bottom left corner of the monitor and is represented as a vector [x y width height]. Finally, the 'Units' property for figure windows and their objects is set to 'normalized' in the PMD. This allows for proper adjustment to monitors of varying resolutions. There are other options for this property such as 'points', 'pixels', and 'inches.'

Axes are used for 2D or 3D plots within a figure window in a GUI. Axes are used extensively throughout the PMD; it allows for a rapid status representation of performance parameters and progress of the performance parameters over time. The most common properties used to define the axes in the PMD are presented in **Table IV**.

Table IV: MATLAB Axes Properties

Property	**Description**
Color	Sets the background color of the axes
Position	Sets the axes position in the figure window

Units	Defines the units of measurement
Xcolor	Sets the color of x-axes outline
Xtick	Sets the xtick mark locations
Ycolor	Sets the color of y-axes outline
Ytick	Sets the ytick mark locations

Uicontrols utilize a "callback" that allows them to perform a task. If a uicontrol has a specified callback, then an action will trigger immediately after the user interacts with it. If the "callback" property has no specified value, then nothing will happen when the user interacts with the uicontrol. There are many uicontrols available in MATLAB. The most common uicontrols utilized in the PMD are presented in **Table V**.

Table V: MATLAB uicontrols

Style	**Description**
Edit	Editable text fields that enables the user to enter or modify text values
Pushbutton	Generate actions when activated; the callback activates immediately after the button is pressed
Text	Displays static text values.

Uicontrols have similar modifiable properties presented in **Table III** and **Table IV**. The remaining properties of uicontrols are described in **Table VI**.

Table VI: MATLAB uicontrols Properties	
Property	**Description**
BackgroundColor	Sets the uicontrol background color
Callback	M-file executed when push-button is pushed down
FontName	Sets font for displaying uicontrol text
FontSize	Sets font size for uicontrol text
FontUnits	Sets font size units for uicontrol text
FontWeight	Sets font weight for uicontrol text
Horizontal Alignment	Sets alignment of uicontrol text
String	Sets uicontrol identifier
Visibility	Sets uicontrol visibility on/off

The PMD requires a total of thirteen M-files required for implementation. Data is shared between all M-files by declaring values as global variables. Each M-file has independent workspaces. This means that variables called within each M-file are stored within each M-File. By declaring variables as global variables, this allows M-files to share the variable between each other. Variables and their stored value allow for rapid access in all components of the PMD. Brief descriptions of each M-file are provided below in the order they are called during implementation:

1. **CREATEFIG1.M** Main calling routine; creates all components of the GUI
2. **EXISTINGMACHINE.M** Loads necessary matrices and stores the

		number of machines in the GUI; creates preference file for future use.
3.	**CALCULATIONS.M**	Performs all necessary calculations to determine status of performance parameters.
4.	**MACHINE.M**	Performs all necessary calculations to determine status of performance parameters; Used when switching between machines
5.	**GRAPH.M**	Plots the I/MR charts; plots the horizontal frequency distribution data; displays statistical summary of a specified performance parameter
6.	**AB.M**	Loads window to apply new chart control limits
7.	**CALCULATE.M**	Calculates and displays new chart control limits based on user input
8.	**APPLY.M**	Applies new chart control limits based on user input to I/MR charts and other associated graphs
9.	**AC.M**	Applies and displays comments about performance parameters
10.	**LEAF_PANEL.M**	Displays each MLC leaf pushbutton and sets the status color of each MLC leaf pushbutton
11.	**LEAFGRAPH.M**	Plots the I/MR charts; plots the horizontal frequency distribution data; displays statistical

		summary of a specified MLC performance parameter
12.	**PRINTREPORT.M**	Creates a pdf report of the I/MR charts of a specified performance parameter
13.	**DATERANGE.M**	Zoom function based on user input of the I/MR charts

The main calling function of the PMD is **CREATEFIG1.M**. This script generates a single figure window that contains all of the components of the program; the PMD is called the "Accelerator PdM Software." Once the figure window is loaded, the user will see the name of the program and a toolbar with three tabs: File, View, and Machines. The 'File' tab consists of three options: Existing Machine, Print Report, and Exit. The 'View' tab consists of one option: Specify Date Range and the 'Machines' tab contains no options until the data becomes loaded into the program. **Figure 9** demonstrates the initial startup session. Other components generated by this script are hidden until the necessary matrices are loaded into the GUI. These components include all pushbuttons and status axes that are related to the performance parameters of medical linear accelerators, I/MR axes and horizontal histograms that are used to monitor the performance parameters of medical linear accelerators, and all callbacks for components which are programmed to perform different tasks.

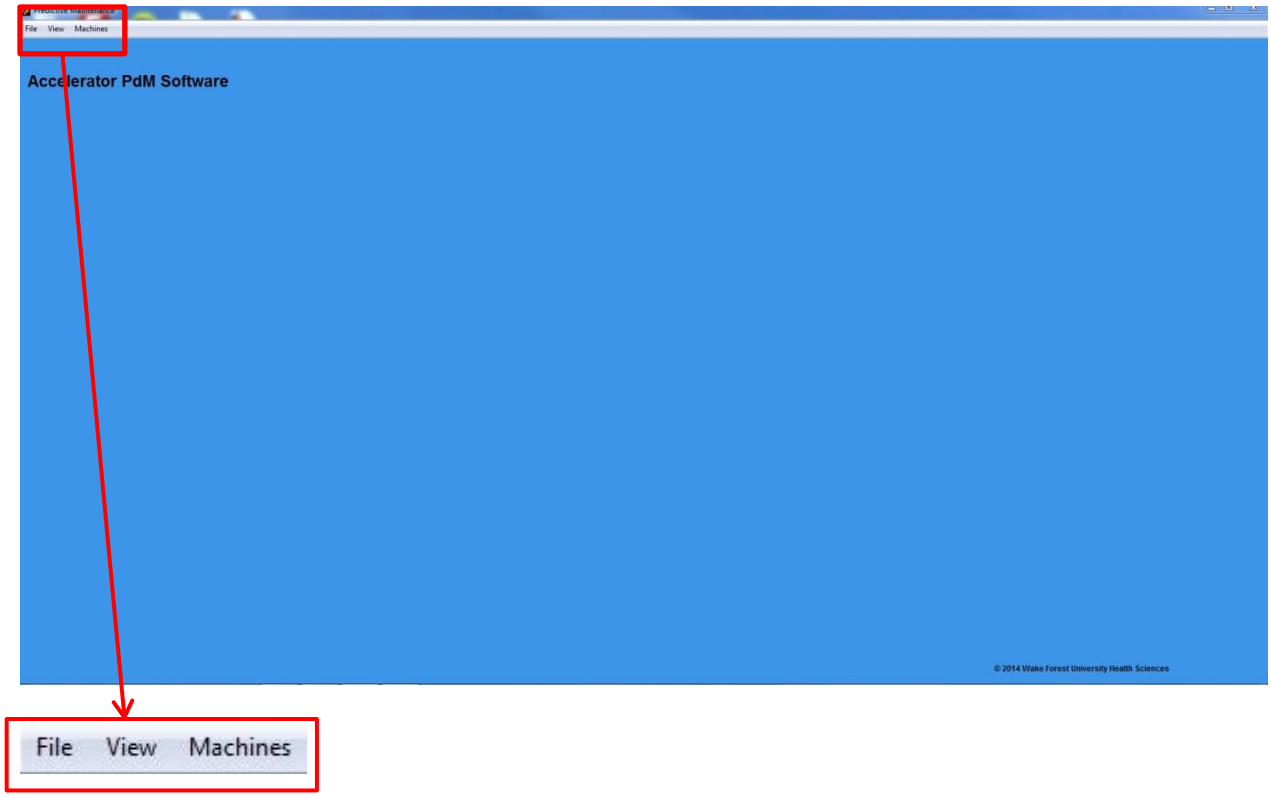

Figure 9. The main GUI window of the PMD. It houses all of the components necessary to develop a PdM system for medical linear accelerators. The PMD has three initial options: File, View, and Machines.

To load data into the GUI, **EXISTINGMACHINE.M** searches for two essential matrices (1) machinedata.mat and (2) SPCMachineName.mat for each machine available per DCP facility (**Figure 10**). The file paths of the two required matrices are then saved in a "PdM.dat" file. This file is a preference file that allows the PMD to preload the data every new session without having to run this script. The name of each machine per DCP facility are then loaded into the 'Machines' tab. This allows for rapid access to each machine per session.

(a)

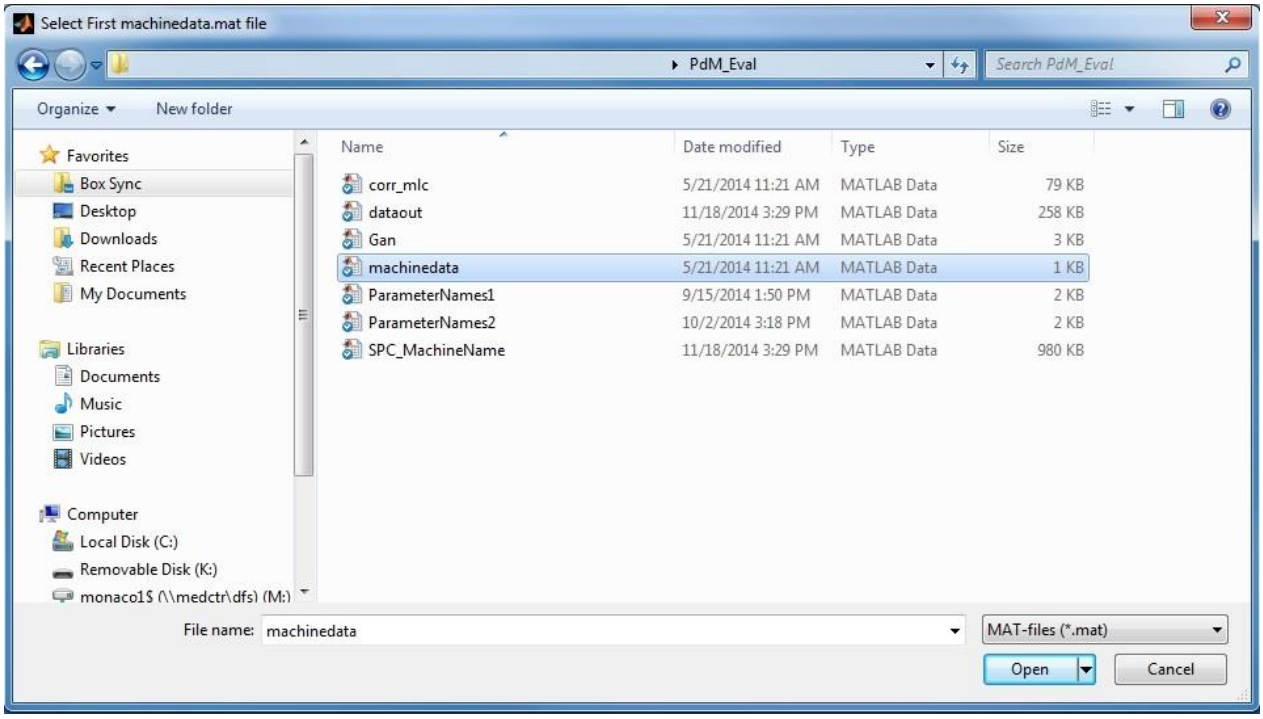

(b)

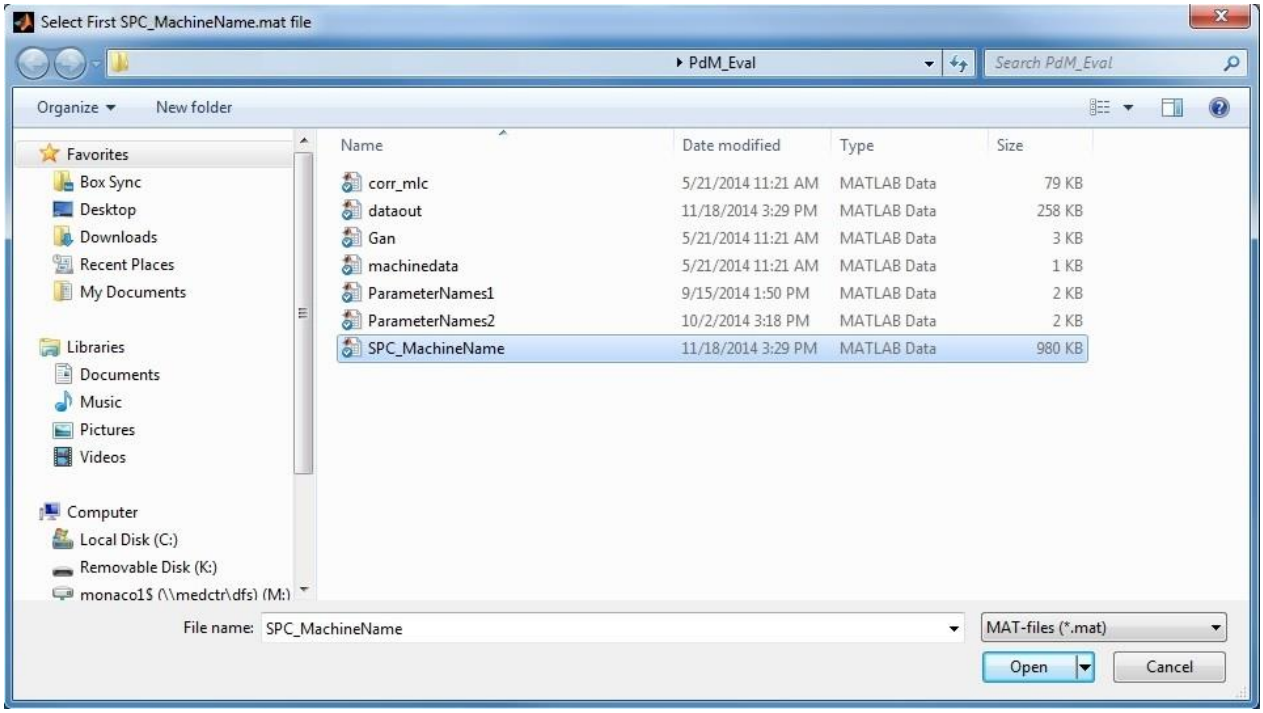

Figure 10. Loading the data into the PMD. The PMD requires two data matrices: machinedata.mat and SPC_MachineName.mat. (a) A window loads and asks the user to

locate machinedata.mat (b) A window loads immediately after and asks the user to locate SPC_MachineName.mat

Once the data is loaded into the PMD, two scripts are called **CALCULATIONS.M** and **MACHINE.M.** Both scripts unhide the first group of pushbuttons that divides the performance parameters into nine major categories; these initial pushbuttons were created when **CREATEFIG1.M** was initiated. Each of these pushbuttons then initiate a second set of pushbuttons that correspond to the performance parameters related to their major category. Axes are placed next to these pushbuttons; these indicate the status of the performance group and/or parameters. Statuses are represented by the following schematic: (1) alarm state is red; (2) warning state is orange; and (3) normal operating state is green. **Figure 11** illustrates this interactive task. Pushbuttons are also coded with a value that corresponds to its placement in the data matrix (SPC_MachineName.mat). Each user-selected input passes the value from one uicontrol to the next uicontrol in the PMD. **CALCULATIONS.M** is the initial function used to determine the status of the performance parameter of the first machine loaded into the PMD. The second script, **MACHINE.M**, has the same capabilities plus one additional capability: toggling between machines. This is meant for DCP facilities that have more than one medical linear accelerator. The user is able to view the status of performance parameters of multiple machines each session. Both scripts also generate a "hot list" of performance parameters. The "hot list" is based on what is considered a critical system for high quality treatment delivery. The most important performance parameters are given a higher priority; thus, if these parameters exhibit nonrandom behavior, then they will be displayed first in this list. The "hot list" displays the top five performance parameters that have the most number of alarms.

(a)

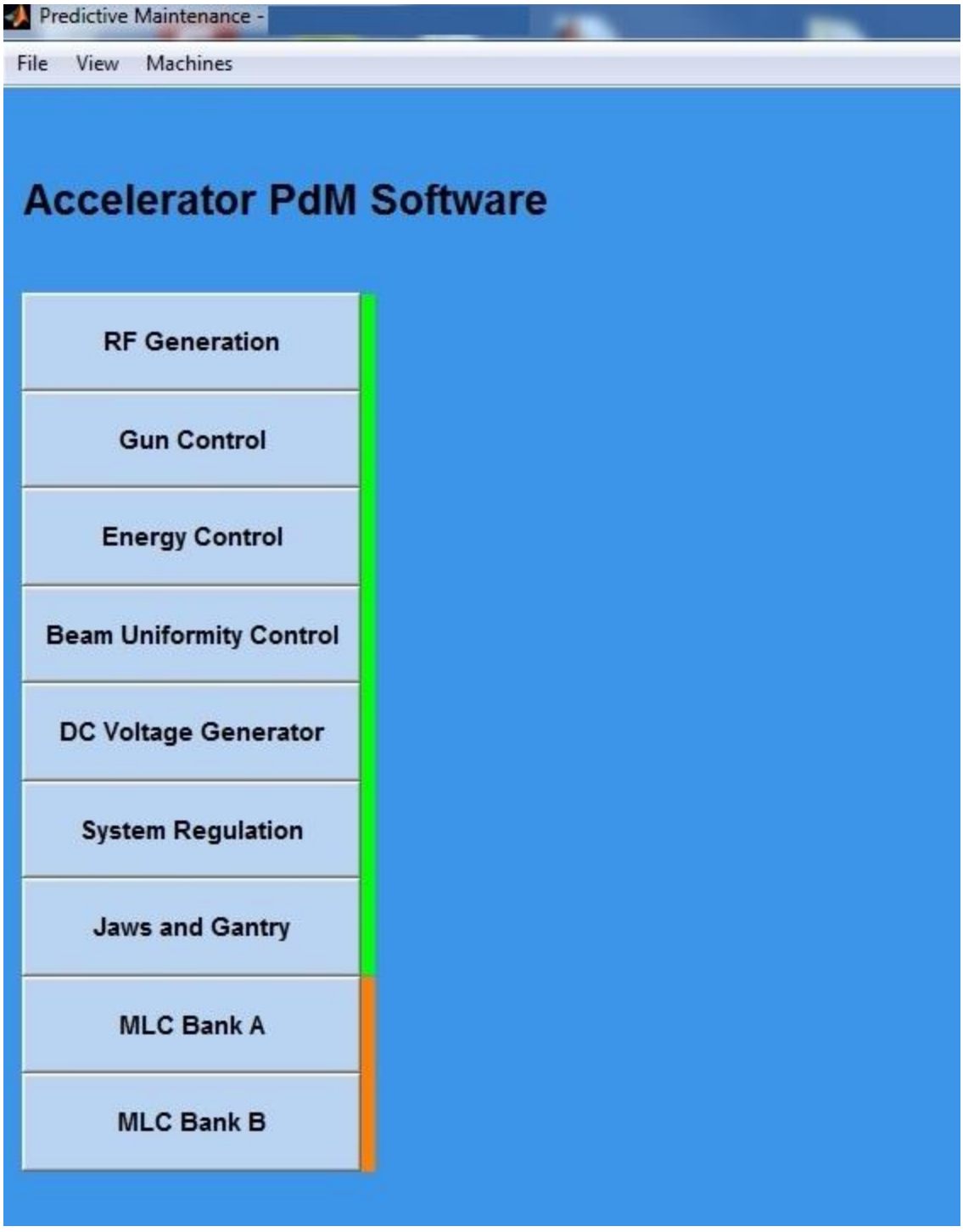
Predictive Maintenance -
File
View
Machines
Accelerator PdM Software
RF Generation
Gun Control
Energy Control
Beam Uniformity Control
DC Voltage Generator
System Regulation
Jaws and Gantry
MLC Bank A
MLC Bank B

(b)

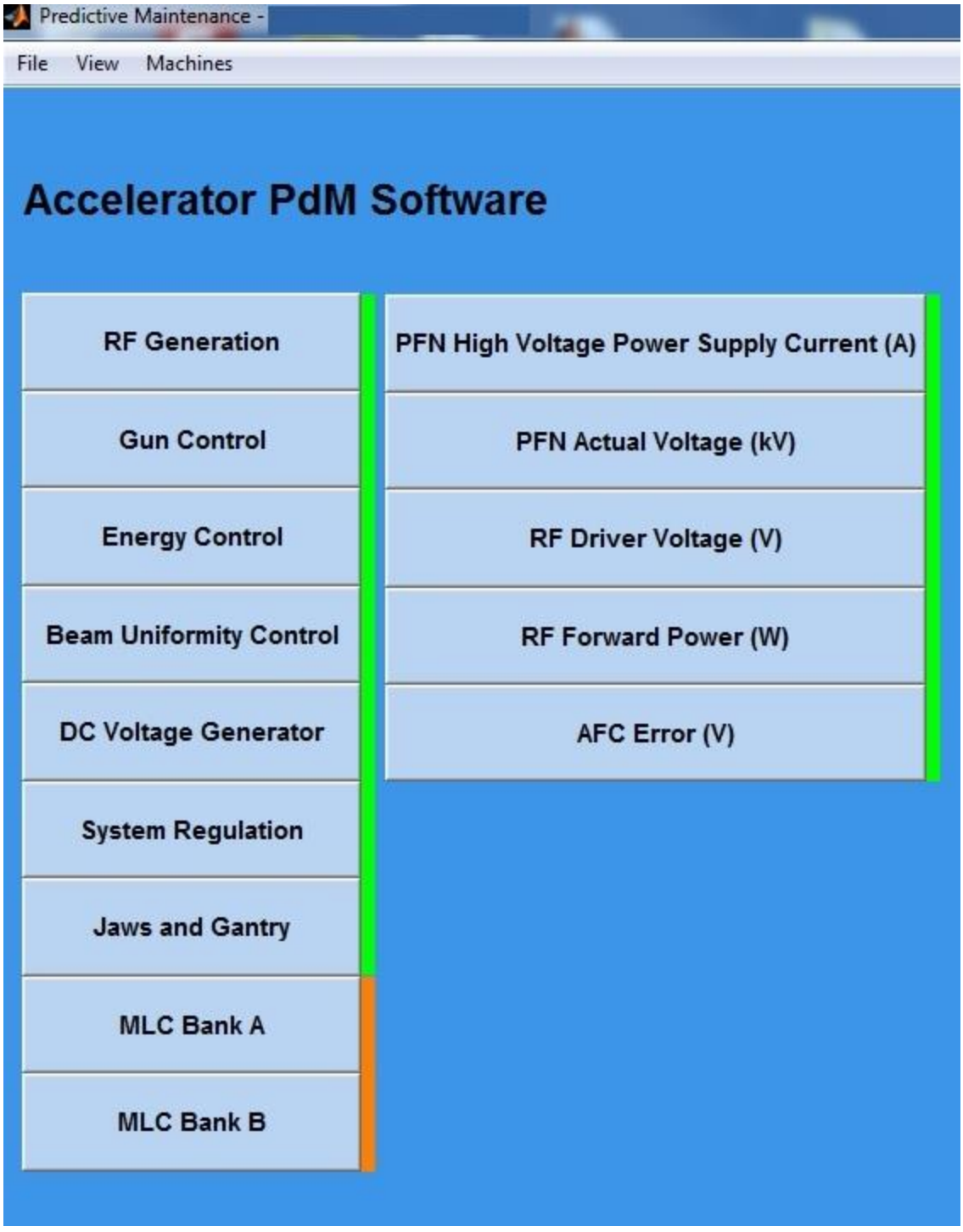

Figure 11. (a) First set of pushbuttons that is seen. These are the nine major categories that contain all of the performance parameters. The operating status is adjacent to the pushbutton. (b) Each pushbutton has a callback that initiates a second set of pushbuttons

that contain the specified performance parameter. In this case, these performance parameter pushbuttons correspond to RF Generation.

GRAPH.M has a number of actions within this function: (1) it plots the I/MR chart of the specified performance parameter; (2) it plots the horizontal frequency distribution of the I chart; (3) it displays a statistical summary of the specified performance parameter; (4) it displays user-generated comments associated with the specified performance parameter; and (5) it reveals two additional features of the PMD: 'Apply New Baseline' and 'Add Comments.' This can be seen in **Figure 12**. **LEAFGRAPH.M** has the same features as **GRAPH.M**; however, this function is used only for MLC leaves.

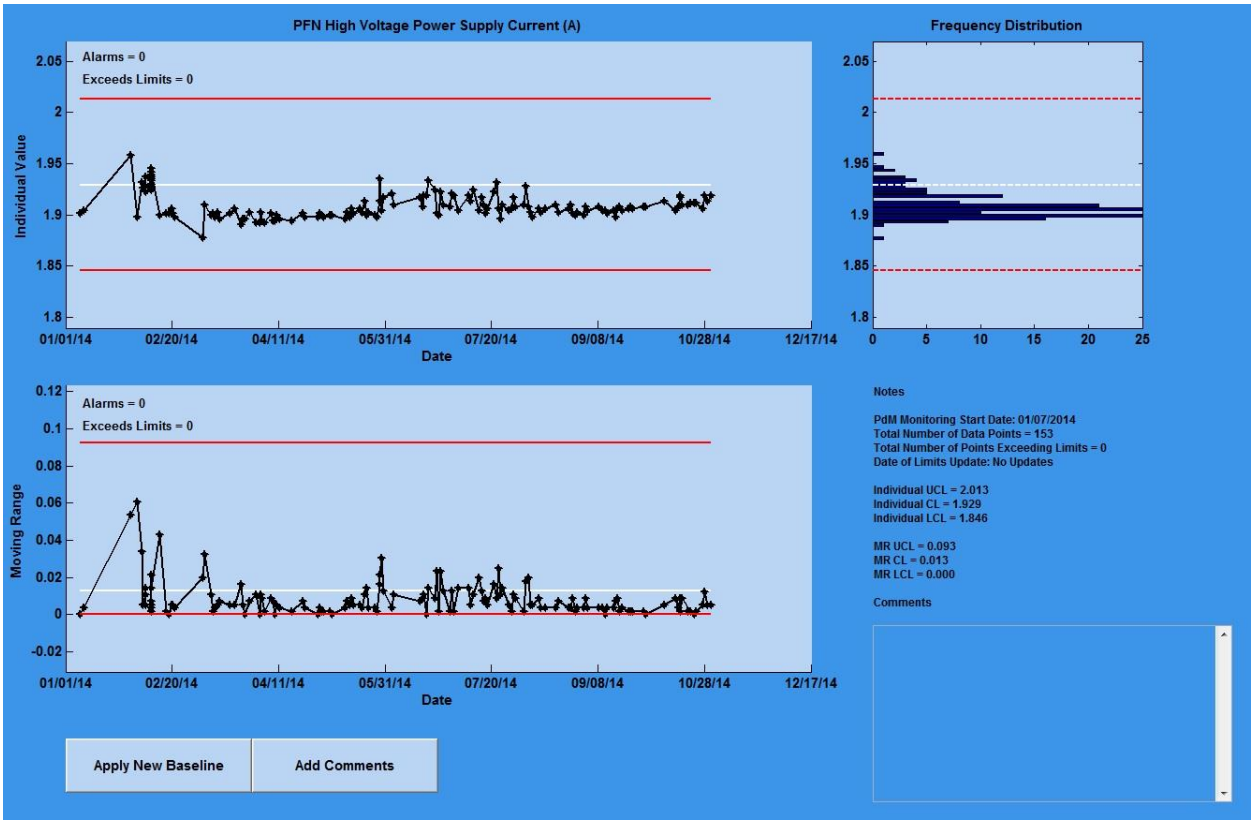

Figure 12. An I/MR chart is generated based on the specified performance parameter. Red lines indicate the chart control limits while the white line indicates the grand mean. A

horizontal frequency distribution is generated in parallel with the individual data set distribution. Other features generated by GRAPH.M are also seen.

AB.M (Apply New Baseline) is accessed at the user's discretion; this is typically utilized when the performance parameter is not in state of statistical control. AB.M allows the user to generate, review, and apply new chart control limits. A figure window loads that asks the user for an input value. **CALCULATE.M** then uses the input value and proceeds to determine the chart control limits to place the performance parameter in a state of statistical control. If the user accepts the new values for the chart control limits, **APPLY.M** is implemented to save these new values in the data matrix and applies them to the I/MR chart and horizontal frequency distribution. **Figure 13** illustrates what is seen by the user.

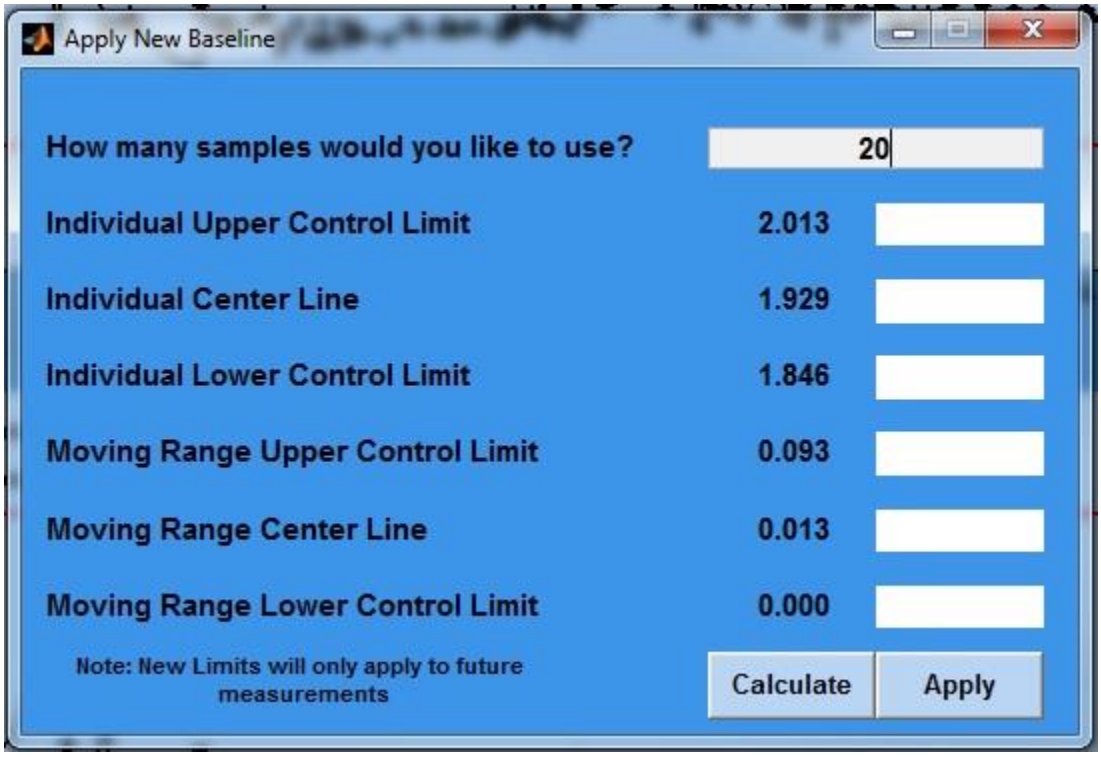

Figure 13. The 'Apply New Baseline' feature that is provided by the PMD.

AC.M (Add Comments) is implemented when the user needs to record notes about the performance parameter. A figure window loads and allows the user to type notes or comments. These comments are then displayed within **GRAPH.M**. **Figure 14** illustrates what is seen by the user.

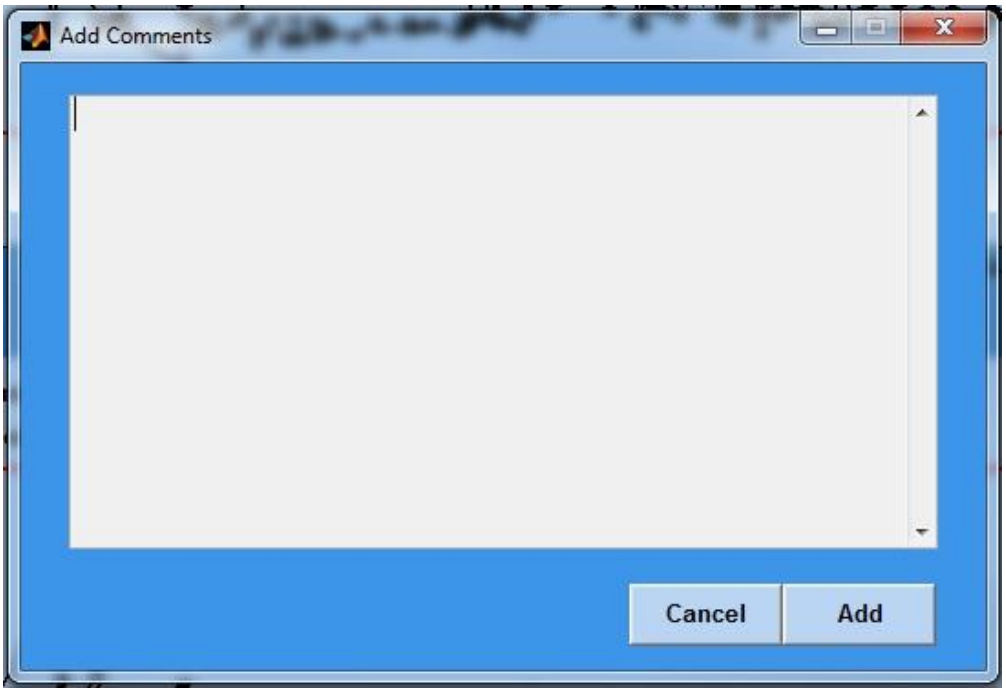

Figure 14. The 'Add Comments' feature that is provided by the PMD.

LEAFPANEL.M is used to display the MLC leaves panel which consists of sixty leaves or pushbuttons. The panel can be accessed by each MLC bank. The panel can be seen in **Figure 15**. Since there are two MLC banks, the panel is used to pass leaf numbers associated with MLC performance such as speeds, CC max values, or LCC max values. Leaf numbers are then passed into **LEAFGRAPH.M**.

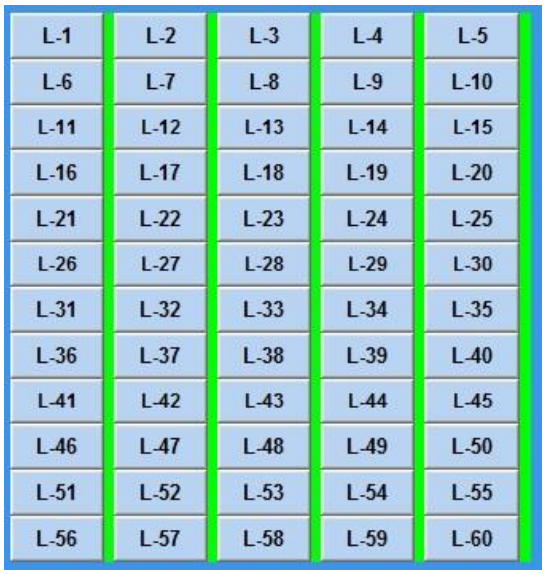

Figure 15. Each MLC leaf has its own pushbutton that allows for rapid interrogation.

The final functions of the PMD are **PRINTREPORT.M** and **DATERANGE.M**. These functions are additional features of the GUI that aid in analyzing the performance of medical linear accelerators. **PRINTREPORT.M** generates a portable document format (PDF) of the I/MR chart of a specified performance parameter. A window loads that displays a preview of the I/MR chart; the user can then print a hard copy of the chart as a reference or record. This feature can be found under the 'File' tab in the main PMD window. **DATERANGE.M** is a function that is an investigational tool. It allows the user to specify a specific date range in which the user would like to view the progress of the performance parameter. A window loads that asks the user to type in a 'Start Date' and 'End Date.' Once the dates are entered, the I/MR chart will then reset its x-axes to the specified date range. If the user needed to reset the x-axes to its original x-axes limits, then the user can push the 'reset' pushbutton. This function can be accessed under the "View" tab in the main PMD window.

V. PdM Effectiveness and Operational Consistency

a. System Dysfunction Detection and Confirmation

The PMD has shown its effectiveness as a user friendly interface displaying the PdM analysis of system functions. The PMD offers features that allow for rapid assessment of performance parameters. These features range from the status lights next to each parameter pushbutton to the visual display of chart control limits. The PMD has coded colors to alert the user of system dysfunction: (1) red is an alarm state; (2) orange is a warning state; and (3) green is a normal state. Moreover, chart control limits become easily visualized. This allows for monitoring of performance parameter progress. Both of these features enhance the PdM analytics; thus, the PMD transforms the PdM model into a powerful and investigative tool in predicting component failure.

Beam Uniformity

The first notable system dysfunction was detected at one of our DCP facilities. The "I" chart for ARC showed a downward trend beginning October 28th, 2013. The ARC entered its first warning state on February 18th, 2014. Initial inquiries by the site physicist indicated that no service had been performed that could have resulted in the changes observed. A review of the daily flatness and symmetry measurements using a two point methodology indicated change of 1.0% from baseline. The ARC entered continuous warning states on March 7th, 2014 until it entered its first alarm state on May 9th, 2014. Data points after that date exceeded the LCL and continued in an alarm state. The beam uniformity (flatness and symmetry) was investigated using a computer controlled water phantom and ion chamber. The radial symmetry was found to differ by 0.8% from the previous annual calibration confirming the "I" chart monitoring. The ARC returned to optimal performance level after adjustments were made by service engineers. This

can be seen in **Figure 16**. The "I" chart detected the drift in the current value 51 days prior to it reaching an alarm state. In this case, the PdM monitoring would have detected the change in the operating parameter early, but did not alarm until almost reaching the TG-142 suggested 1% constancy level [28]. In addition, the control limits ensured no alarm state occurred prior to the TG-142 suggested 1% constancy level.

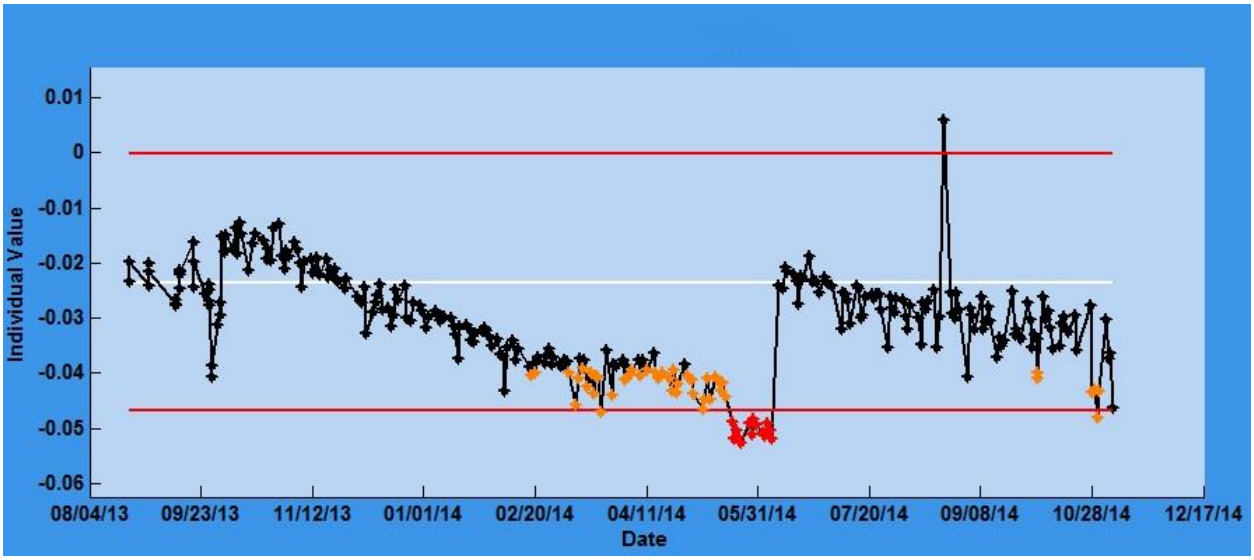

Figure 16. The progress of the ARC at one of our DCP facilities. Continuous monitoring following service adjustments indicates beam steering was restored to its baseline value.

Gantry Position Accuracy

The second notable system dysfunction was detected at another one of our DCP facilities. The "I" chart for Gantry Location of Cross Correlation Max Value (GLCC) showed a downward trend beginning June 6th, 2014. The GLCC then proceeded to enter numerous alarm states starting June 23rd, 2014 and persisted until September 30th, 2014. The DCP facility physicist delivered the daily QA treatment and noted irregular gantry movement during delivery. There was visible recoil from its original position and the treatment terminated on an interlock fault. The gantry was unable to quickly halt its movement during high accelerations and decelerations

as required by the QA treatment. Since one of the characteristics of the VMAT treatment delivery process is continual assessment of dose accumulation, MLC position, and gantry location, the actuation of the interlock indicated that the gantry was unable to perform at an optimal level. The gantry's rotational accuracy exceeded the chart control limits generated by PdM analytics (cross correlation equivalent limits of ± 0.15 degrees) and accuracy specifications set by the manufacturer (≤ 0.3 degrees). This can be seen in **Figure 17.** The gantry performance returned to optimal levels after adjustments were made by service engineers. PdM monitoring would have detected the change in gantry performance at an earlier instance and prompted immediate maintenance before September 30th, 2014.

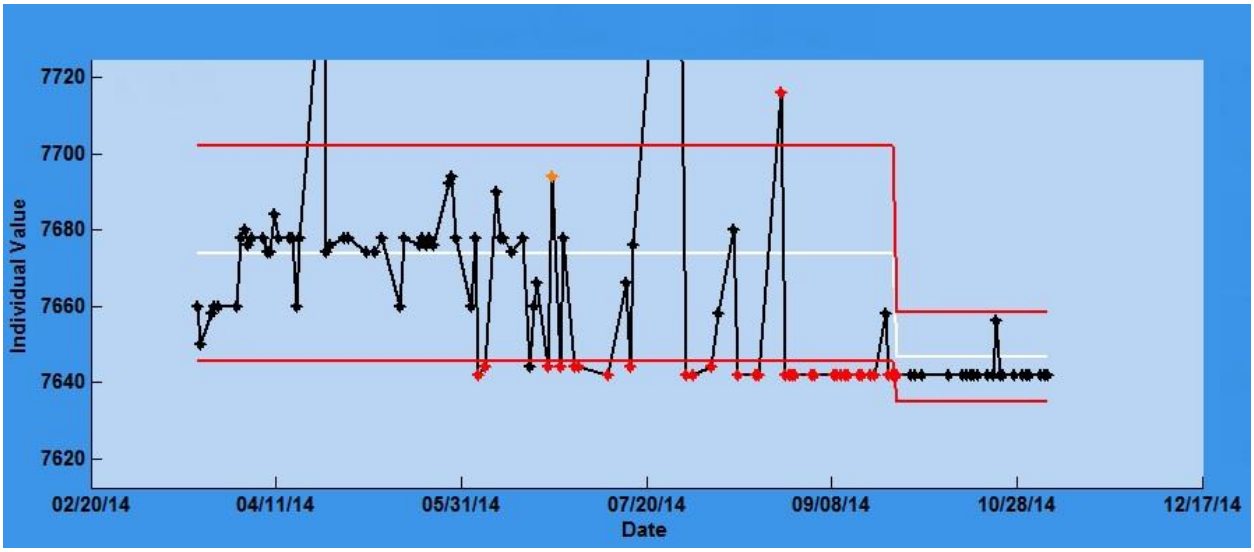

Figure 17. The progress of the GLCC at one of our DCP facilities. New chart control limits needed to be revised when the process operated at a new baseline value.

MLC Motor

The last notable system dysfunction was detection of a failing MLC motor, specifically MLC leaf 26 in carriage bank B. During a service call for MLC fault, a pulse width modulation (PWM) analysis revealed that there were abnormally large DC pulses running through the motor drives. A PWM analysis is used to assess the performance status of MLC leaf positioning by

applying DC pulses directly to the motor windings until each motor drives its individual leaf 2.0 mm beyond initial set positions [30]. The "I" chart for MLC leaf 26B in CC Max Value noted that the leaf was above its normal operating performance for several months. The first initial warning and alarm were on February 5th, 2014 and April 3rd, 2014, respectively. The CC Max Values of MLC leaf 26B proceeded to enter numerous warning states after this date; thus, high DC pulses were applied to this leaf to correct its position in the carriage. PdM monitoring would have detected the high DC pulses being sent to the leaf during its initial progress monitoring. The motor was replaced on October 21st, 2014 and the process returned to normal operating status. This can be seen in **Figure 18**.

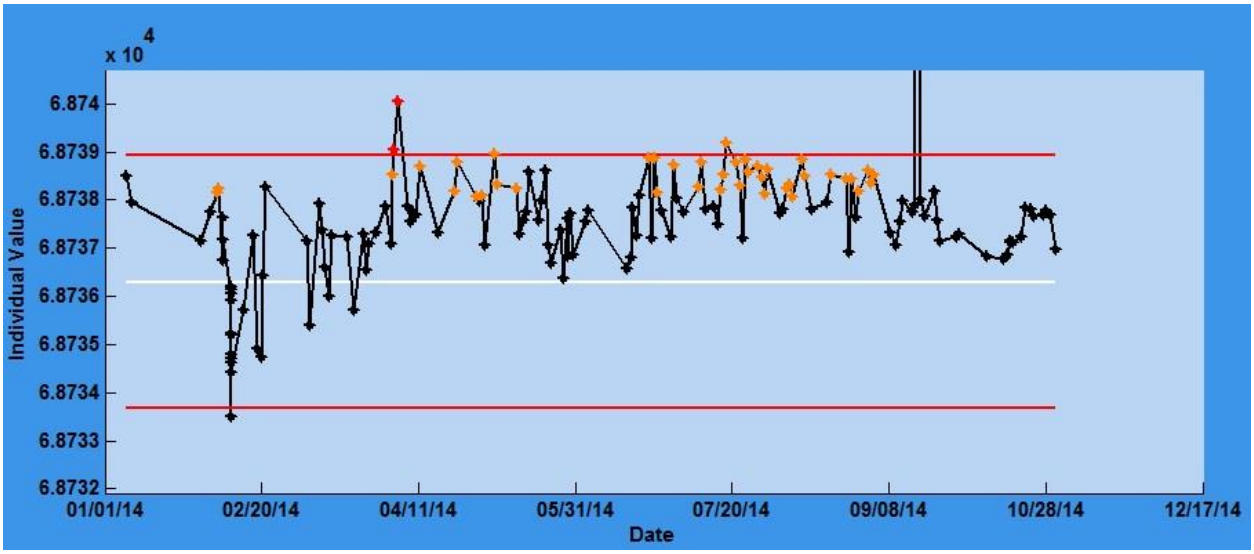

Figure 18. The progress of the CC Max Values of MLC Leaf 26 in carriage bank B. PdM monitoring revealed that the process was deviating for an extended period of time before its pre-emptive maintenance on October 21st, 2014.

The PMD has shown promise in facilitating the detection of erratic behavior in linear accelerators. The key value of the PMD is its ability to materialize PdM analytics that has demonstrated its utility in predicting and preventing component failure. Users can monitor each performance parameter in an ergonomic interface. The previous examples serve to justify, not

only its utility as a practical interface, but its effectiveness as a predictive maintenance tool. Extensive analysis over time will better determine its overall value and usefulness.

b. Operational Consistency

The increasing complexity of machines requires that its internal components are subjected to numerous inspections and analyses. Each investigation ensures that its internal components are operating at a certain "tolerable" level before being used. Linear accelerators are highly complex machines that require meticulous checks to ensure its efficiency in the clinic. Thus, their internal components must operate at a specific optimal level. This specificity drives the theory that linear accelerators and its components perform at similar levels when produced by the same manufacturer. In this thesis, operational consistency and/or constancy are investigated to draw a conclusion about the performance states of TrueBeam linear accelerators.

Performance parameters across all DCP accelerators were subjected to an analysis of variance (ANOVA) to determine if there were differences between each of their parameter means. The assumptions of ANOVA are that the variances are independent, normal, and homogeneous. Since each DCP was asked to deliver the QA treatment delivery at different points in time, each TrueBeam accelerator monitored had an unequal amount of treatment deliveries. Thus, a ranked ANOVA was used because the ANOVA assumption of normality (equal sample sizes) was violated [31]. In the ranked ANOVA, each original data point value is replaced by a rank (from 1 for the smallest to *N* for the largest) [31]. Ranking improves the data set by adding robustness to non-normal errors (due to unequal sample sizes) and resistance to outliers [31]. All performance parameters were compared across all DCP accelerators using a ranked ANOVA. **Table VII** summarizes the initial results of statistical differences.

Table VII: Statistics for Important Performance Parameters in TrueBeam systems (7 linear accelerators – TB and STX models)			
Performance Parameter	**Range**	**Maximum Difference**	**P-Value**
Angle Radial Current (A)	-0.063 – 0.111	0.175	< 0.00001
Angle Transverse Current (A)	-0.127 – 0.145	0.272	< 0.00001
Position Angle Current (A)	-1.264 – 0.273	1.536	< 0.00001
Position Transverse Current (A)	-0.476 – 0.759	1.234	< 0.00001
Gantry Speed 2 (Deg/sec)	5.534 – 5.841	0.307	< 0.00001

The results of the ranked ANOVA indicate that all TrueBeam performance parameters monitored were statistically different (p-value < 0.00001). **Table VII** depicts the five of the most important treatment delivery parameters but is representative of all the performance parameters that were monitored. The "range" is the minimum and maximum mean value of that specific performance parameter and the "maximum difference" is the difference between the maximum and minimum mean value. The initial results indicate that each accelerator parameters operate collectively at a distinct and consistent value.

To further examine this theory, we perform the same analysis on the STX model of accelerators. **Table VIII** summarizes the results of this case. Again, it was determined that all STX TrueBeam performance parameters were statistically different (p-value < 0.00001). One interesting observation was that the maximum differences between the same classes of accelerators were less than the maximum differences between all classes of accelerators.

Table VIII: Statistics for Important Performance Parameters in TrueBeam systems (4 linear accelerators – STX Models)			
Performance Parameter	**Range**	**Maximum Difference**	**P-Value**
Angle Radial Current (A)	-0.063 – 0.054	0.117	< 0.00001
Angle Transverse Current (A)	-0.008 – 0.088	0.096	< 0.00001
Position Angle Current (A)	-1.182 - 0.273	1.455	< 0.00001
Position Transverse Current (A)	-0.214 – 0.759	0.973	< 0.00001
Gantry Speed 2 (Deg/sec)	5.534 – 5.683	0.148	< 0.00001

We also examined the differences between two STX accelerators that were manufactured and commissioned in series. This analysis determined that performance parameters within STX TrueBeam systems with consecutive serial numbers were statistically different (p-value < 0.00001). Maximum differences in these parameters were further narrowed. **Table IX** summarizes the results of this investigation.

Table IX: Statistics for Important Performance Parameters in TrueBeam systems (2 linear accelerators – STX consecutive serial numbers)		
Performance Parameter	**Maximum Difference**	**P-Value**
Angle Radial Current (A)	0.07	< 0.00001
Angle Transverse Current (A)	0.012	< 0.00001
Position Angle Current (A)	1.036	< 0.00001
Position Transverse Current (A)	0.475	< 0.00001
Gantry Speed 2 (Deg/sec)	0.01	< 0.00001

In summary, a ranked ANOVA proved that the performance parameters of linear accelerators monitored are statistically different; the monitored performance parameters were distinct from one another. While each accelerator meets treatment performance requirements (Beam Flatness/Symmetry and Uniformity, Gantry Speed, etc), the performance parameters are consistently different.

Performance parameters were then investigated in greater detail to determine how "different" they performed at each DCP accelerator. To depict the differences, the mean of the "I" chart value was plotted for each DCP accelerator for the same parameters including the gantry CC **(**note that the DCP accelerators are listed starting with the consecutively manufactured STX TrueBeams followed by the remaining STX TrueBeams and finally the other TrueBeam accelerators) (**Figures 19-24).** It was visually determined that for each performance parameter, each DCP accelerator had distinct mean values. The ARC (**Figure 19**), ATC (**Figure 20**), PRC (**Figure 21**) and PTC (**Figure 22**) show that the mean values were consistently different. In addition, an interesting observation was that the Gantry Speed 2 and CC Max Values performed at a relatively equal level (**Figure 23-24**). There were at least two pairs of TrueBeam accelerators with similar mean speeds and CC max values. TrueBeam accelerator parameters, whether of the same or different model, operate at a unique value.

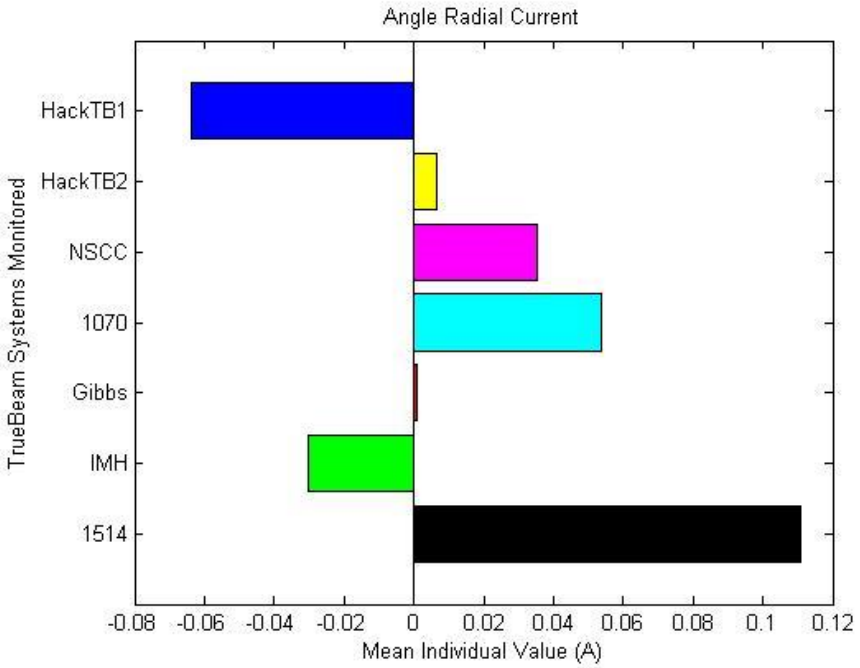

Figure 19. This figure depicts the mean of all "I" chart values for each DCP accelerator for the ARC. The mean values show that each TrueBeam parameter is distinct across each DCP accelerator.

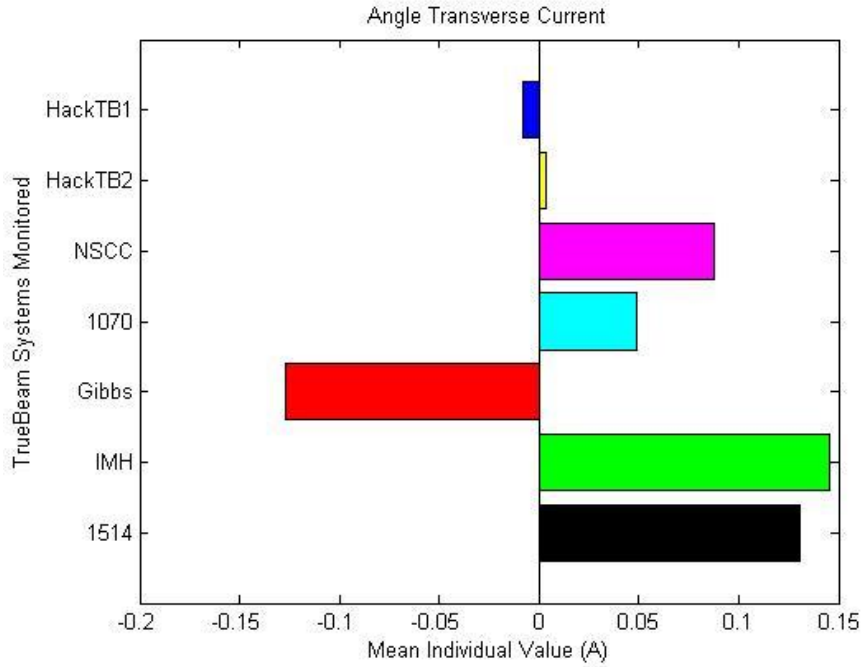

Figure 20. This figure depicts the mean of all "I" chart values for each DCP accelerator for the ATC. The mean values show that each TrueBeam parameter is distinct across each DCP accelerator.

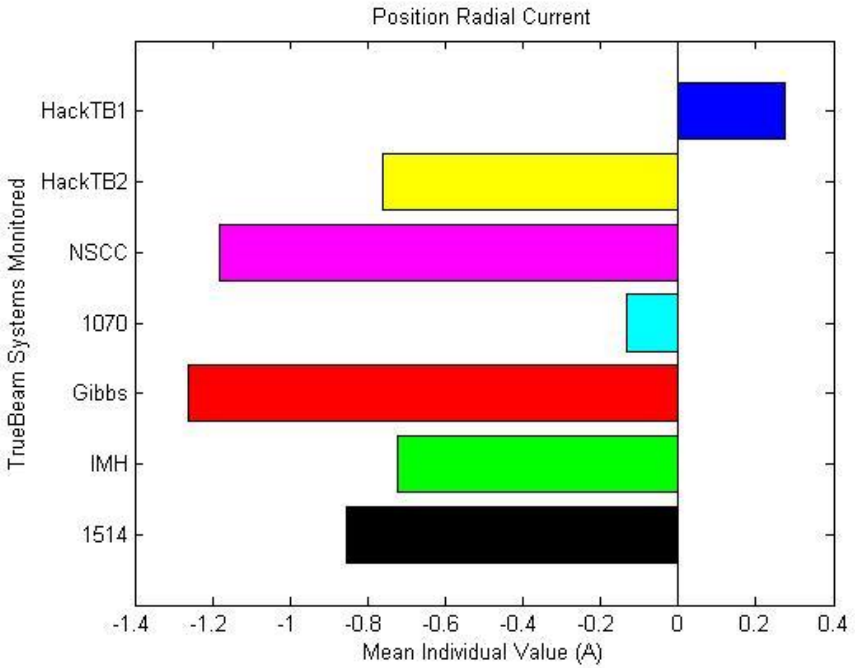

Figure 21. This figure depicts the mean of all "I" chart values for each DCP accelerator for the PRC. The mean values show that each TrueBeam parameter is distinct across each DCP accelerator.

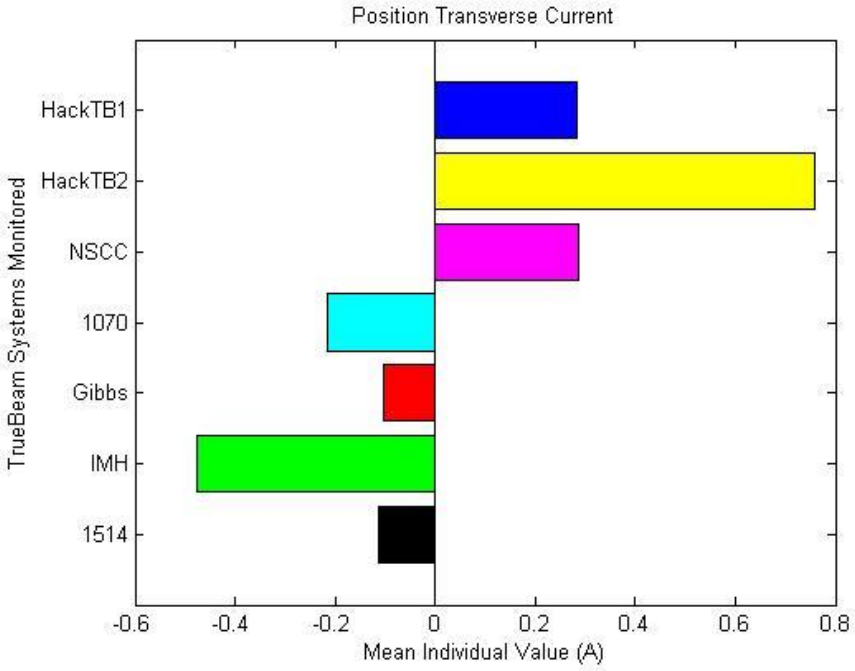

Figure 22. This figure depicts the mean of all "I" chart values for each DCP accelerator for the PTC. The mean values show that each TrueBeam parameter is distinct across each DCP accelerator.

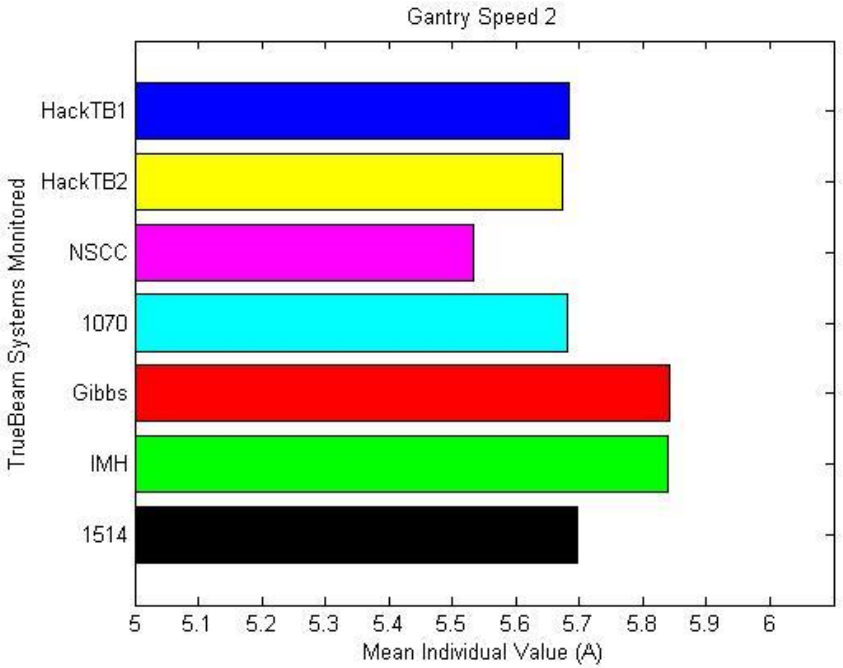

Figure 23. This figure depicts the mean of all "I" chart values at each DCP accelerator for Gantry Speed 2. The mean values show that each TrueBeam parameter is distinct across each DCP accelerator.

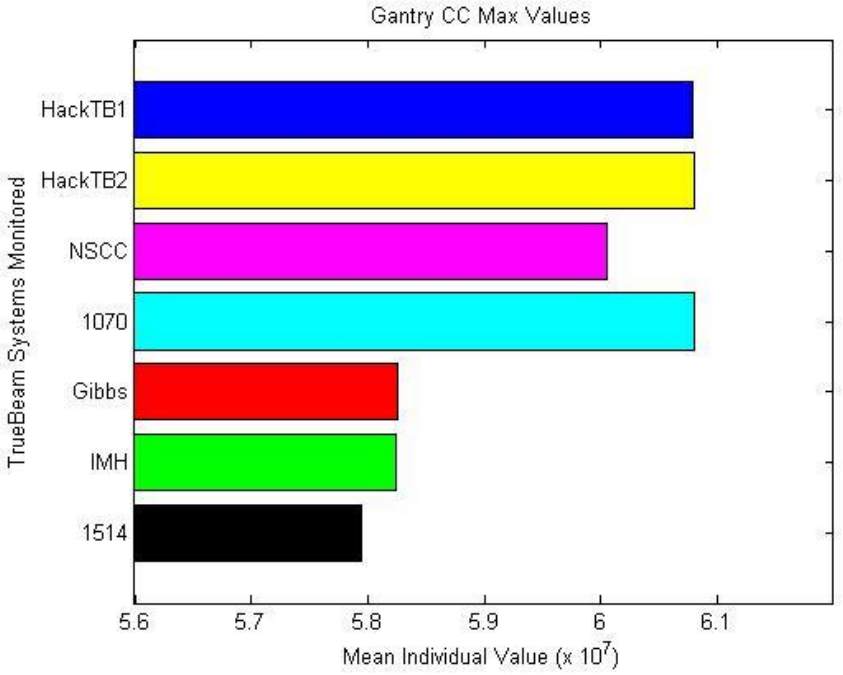

Figure 24. This figure depicts the mean of all "I" chart values for each DCP accelerator for the Gantry CC Max Values. The mean values show that each TrueBeam parameter is distinct across each DCP accelerator. Most accelerators had similar mean values.

Another visual investigation to further test this theory was examining how each performance parameter deviated from an overall mean value. This interpretation provides a method of determining whether a performance parameter operates at a single, specific value. Three systems critical to the accurate delivery of any accelerator based radiotherapy treatment: beam uniformity, gantry position fidelity, and MLC position fidelity are displayed in **Figures 26-27**. An overall mean value was calculated for each performance parameter in these systems across all DCP accelerators. It was then used to extract the residuals from the overall mean value for each DCP accelerator. It was visually determined that for each performance parameter within the chosen accelerator operated at a unique value specific to the TrueBeam. Beam uniformity control parameters showed widespread deviations from the overall mean value for a specific parameter. The deviations in the PRC and PTC were larger than the other beam uniformity control parameters (**Figure 25**). Gantry and MLC speed and CC max values and LCC max values parameters showed a similar result (**Figure 26 – 27**). Thus, parameters within a TrueBeam accelerator operate at a unique and distinct value.

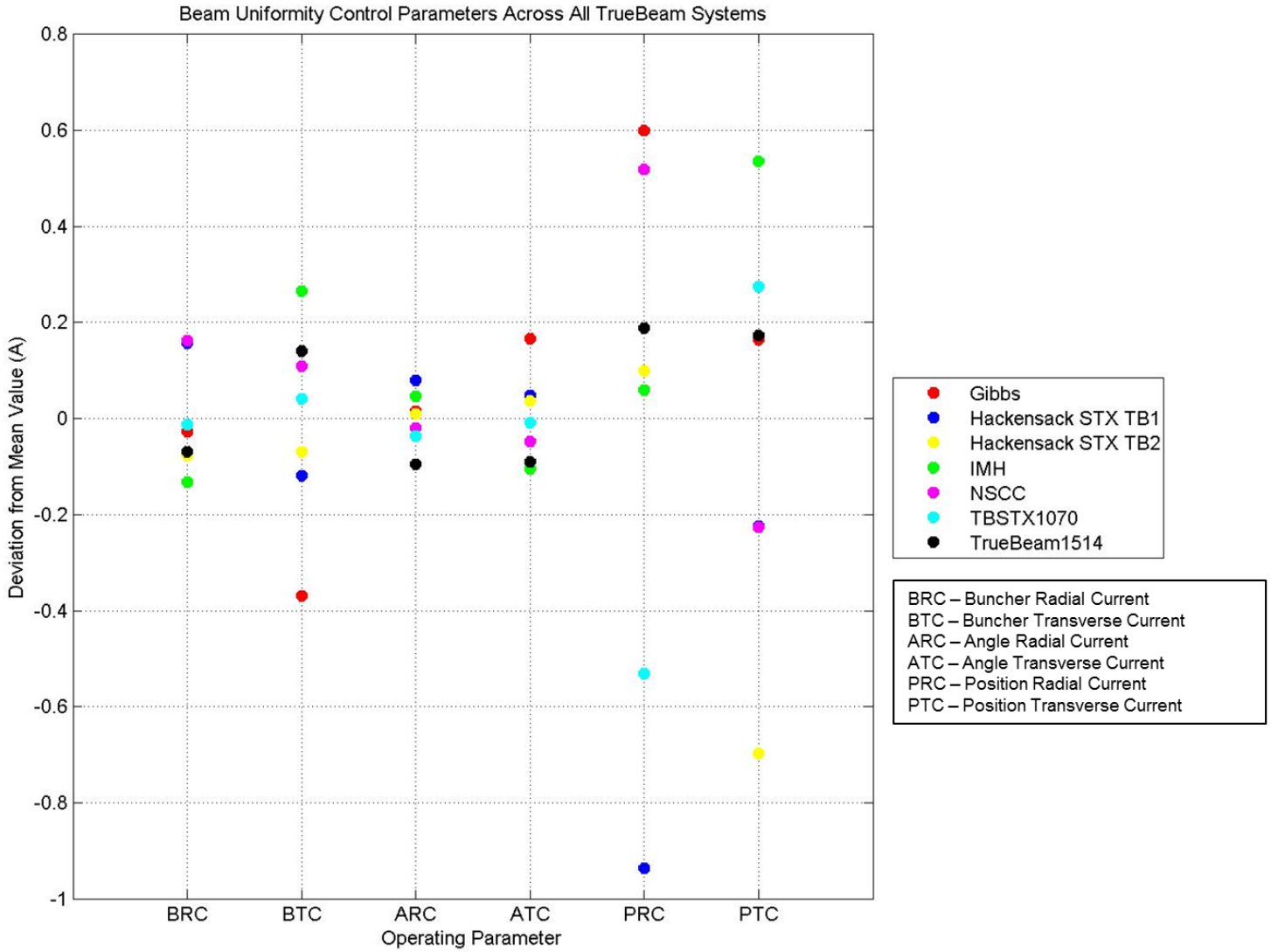

Figure 25. This figure depicts the deviations from an overall mean value for each performance parameter in Beam Uniformity Control. The deviations show that each TrueBeam parameter operates at distinct values for each DCP accelerators.

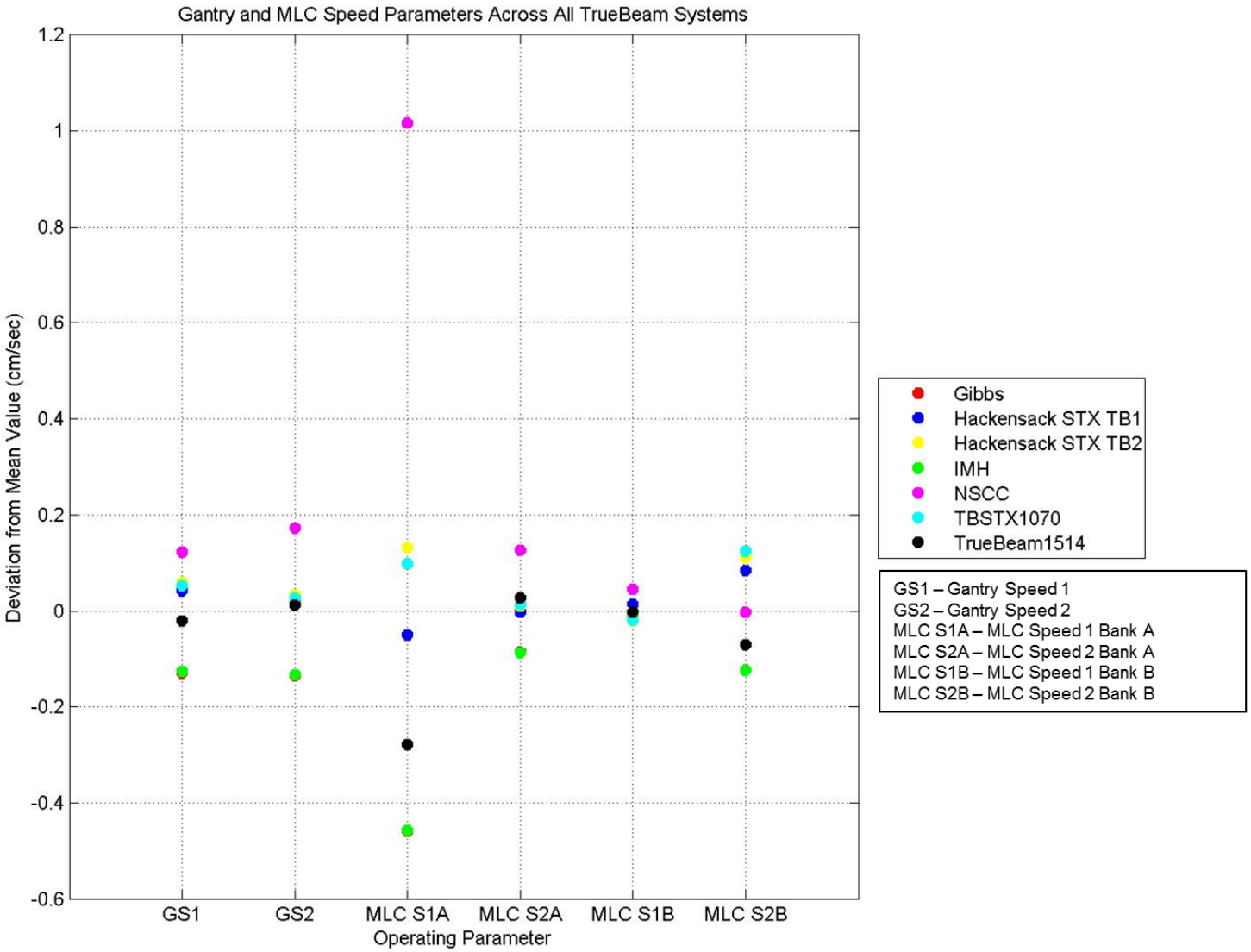

Figure 26. This figure depicts the deviations from an overall mean value for each performance parameter in Gantry and MLC Speed Parameters. The deviations show that each TrueBeam parameter operates at distinct values for each DCP accelerators.

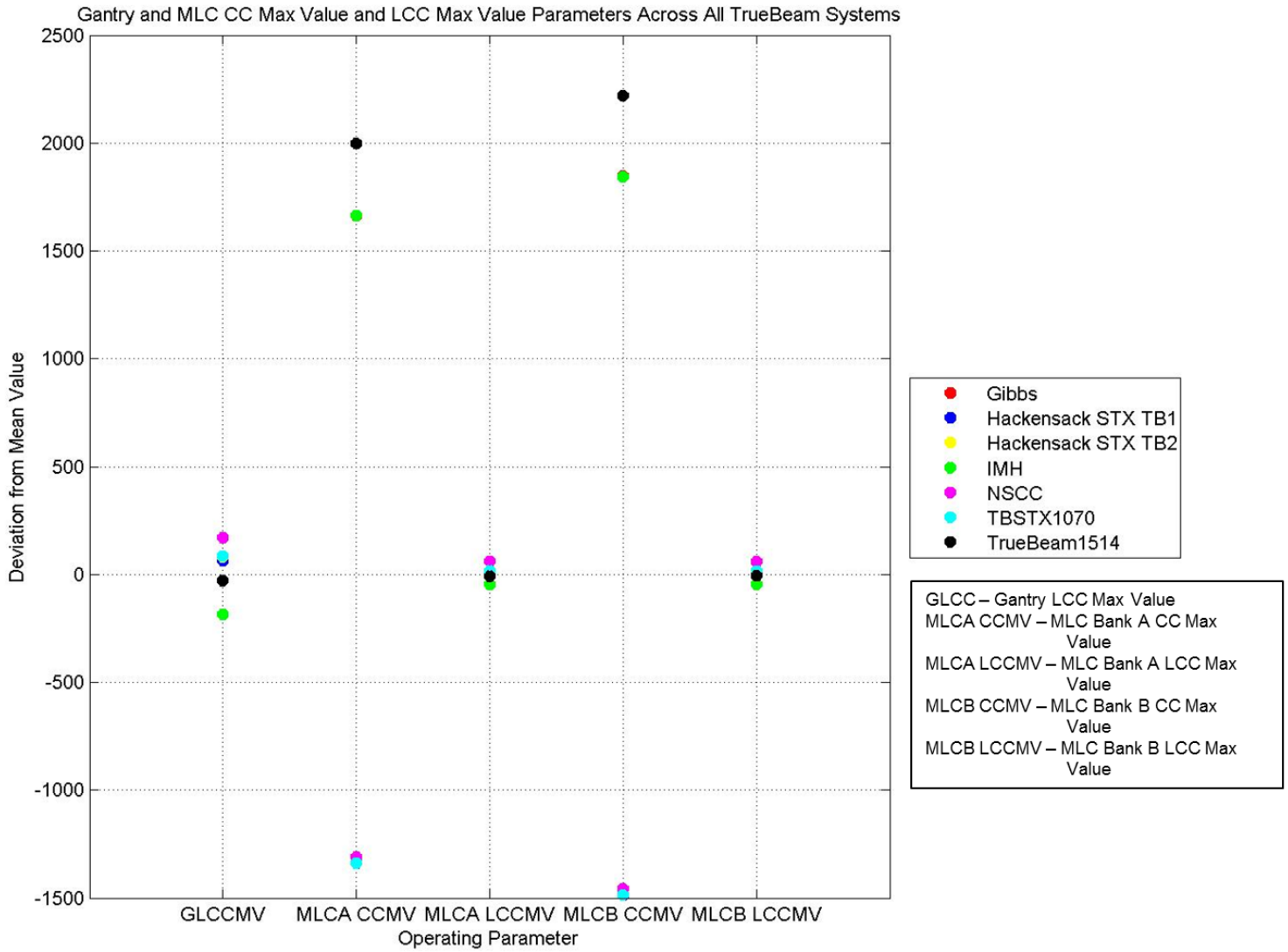

Figure 27. This figure depicts the deviations from an overall mean value for each performance parameter in Gantry and MLC CC Max Value and LCC Max Value Parameters. The deviations show that each TrueBeam parameter operates at distinct values for each DCP accelerators.

A final test of the theory was the investigation of the PdM limit range. This inquiry depicts the operating window in which the parameter is performing for each DCP accelerator. PdM analytics has shown that it is effective at specifying a window in which the parameter is in a state of statistical control; thus, they can be used as a comparison metric to determine if there are overlapping operating windows (**Figures 28-32**). Each parameter had a unique operating window characteristic of that particular TrueBeam system; there was minimal overlap when comparing all DCP accelerators. Thus, linear accelerators and its components perform at differing levels when produced by the same manufacturer. TrueBeam linear accelerators are statistically and operationally different. More importantly, each accelerator meets the clinical treatment performance specifications.

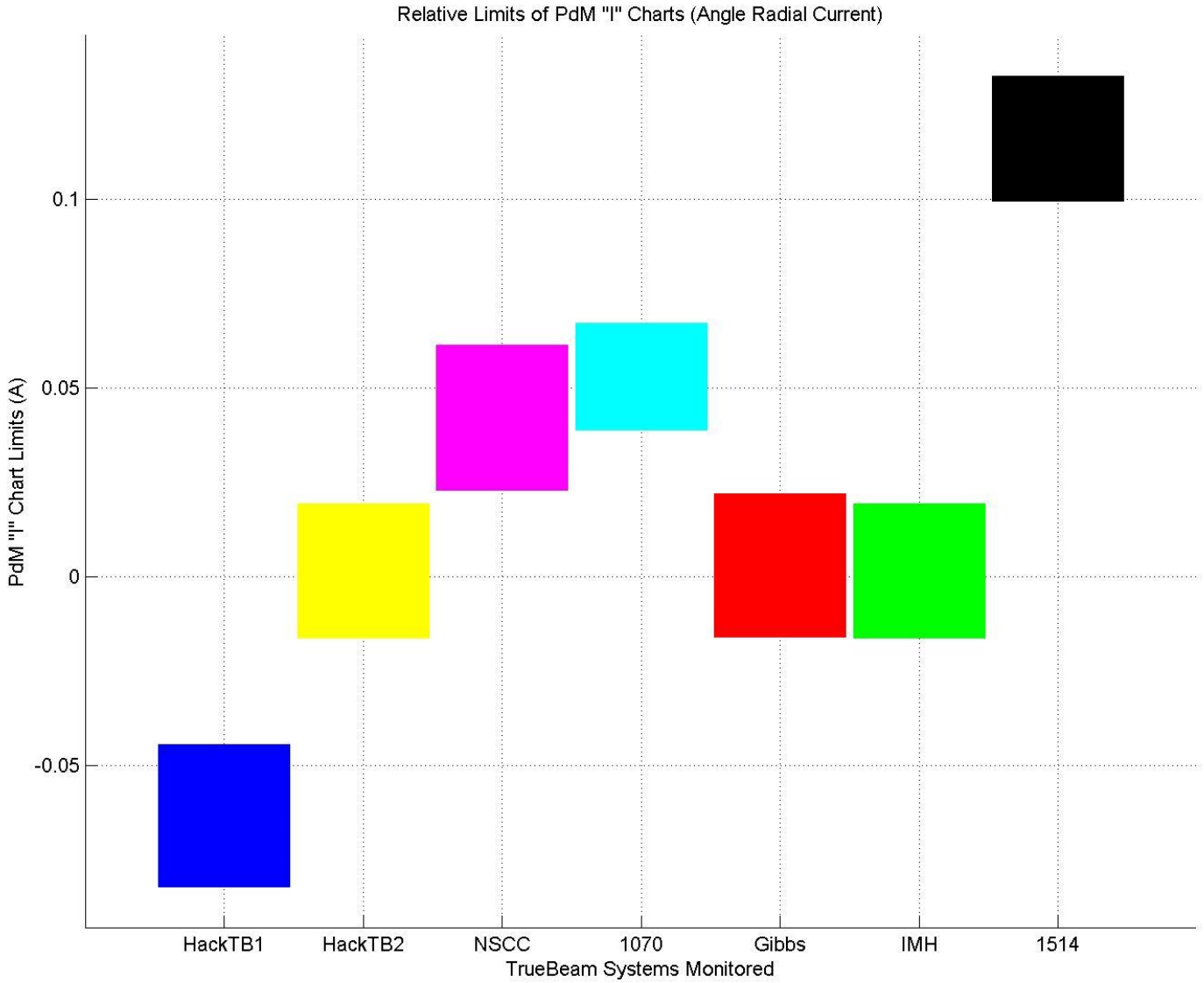

Figure 28. This figure depicts the control limits of the "I" chart for each DCP accelerator for ARC. The control limits show that each DCP accelerator has its own operating window.

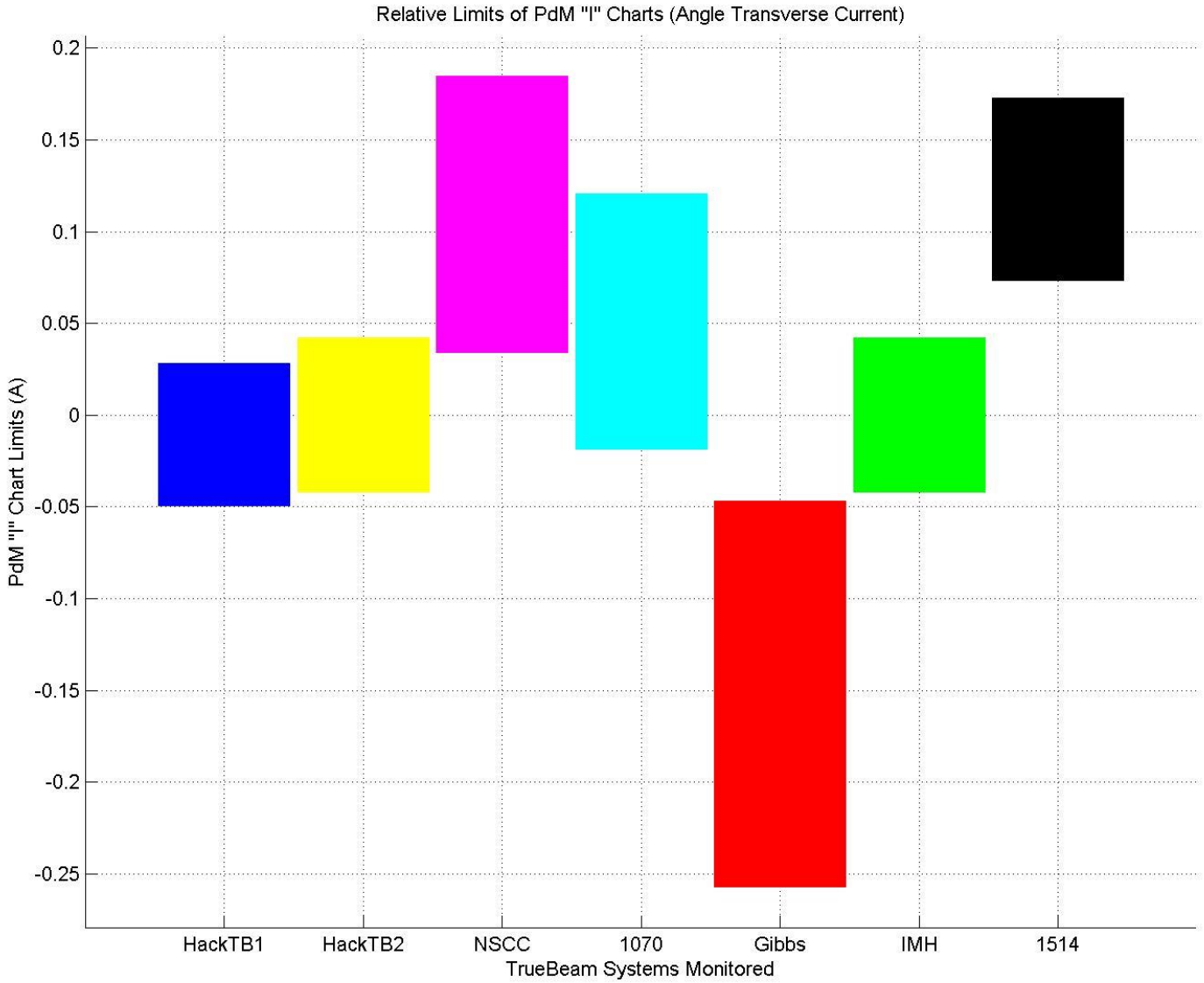

Figure 29. This figure depicts the control limits of the "I" chart for each DCP accelerator for ATC. The control limits show that each DCP accelerator has its own operating window.

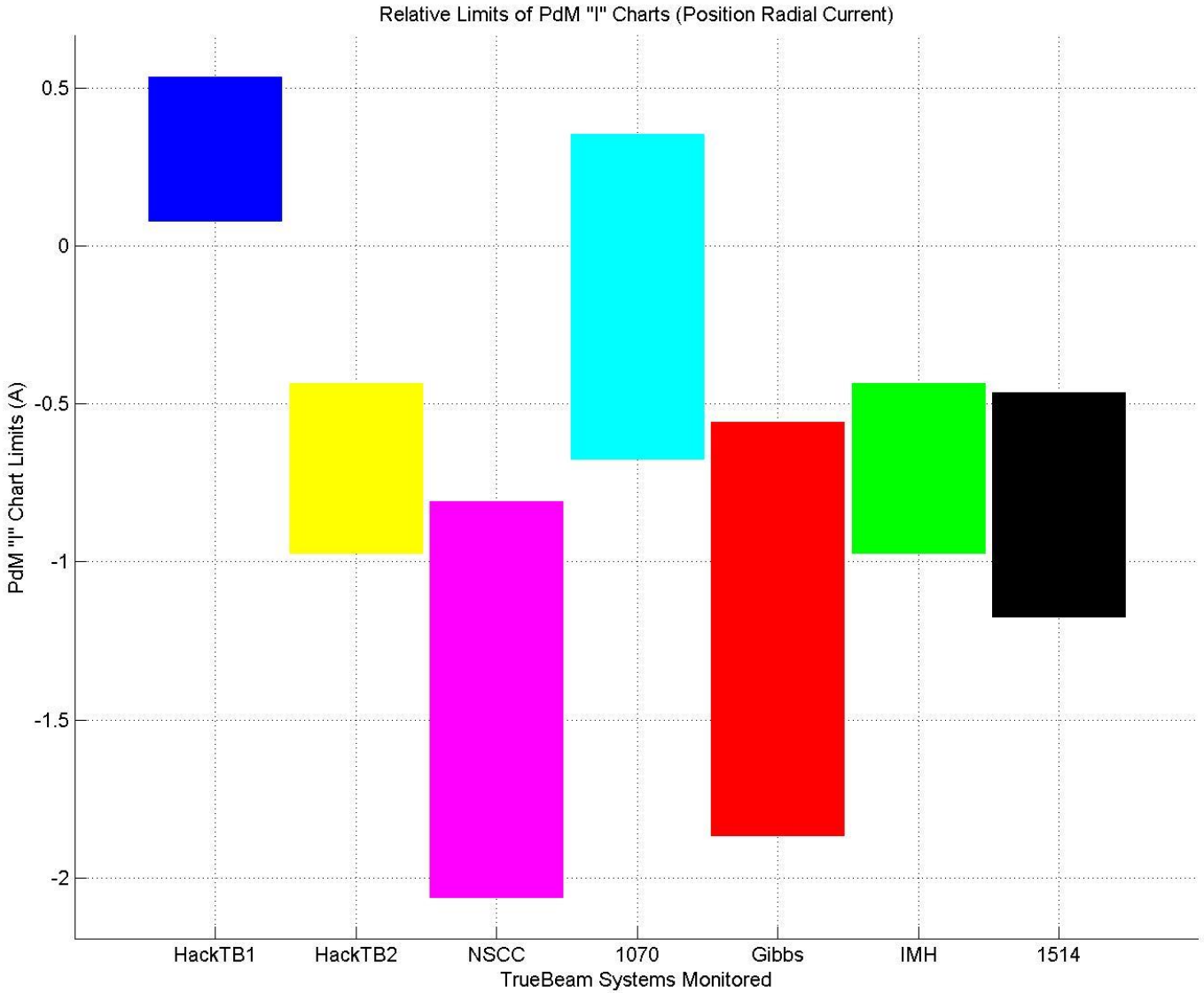

Figure 30. This figure depicts the control limits of the "I" chart for each DCP accelerator for PRC. The control limits show that each DCP accelerator has its own operating window.

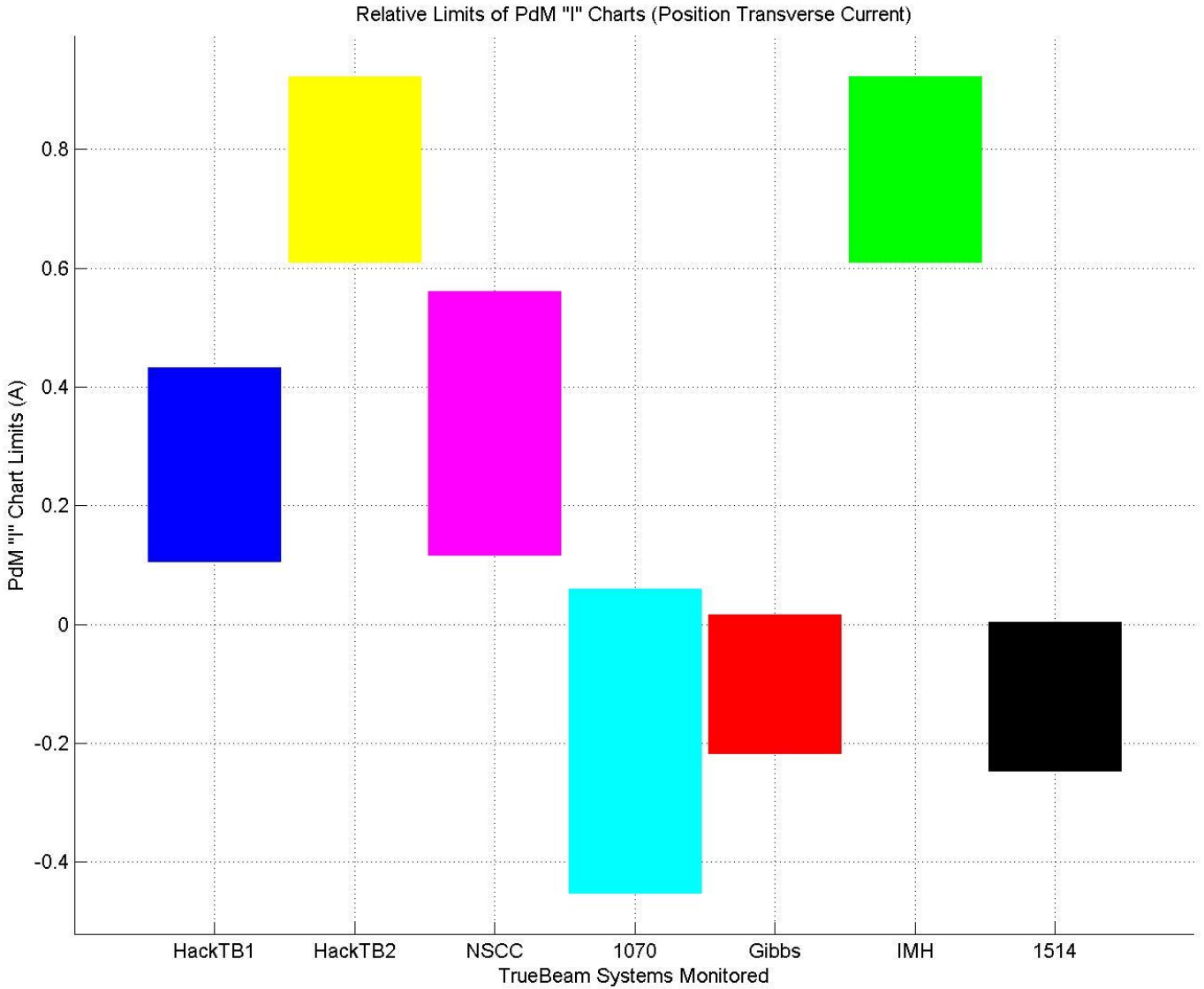

Figure 31. This figure depicts the control limits of the "I" chart for each DCP accelerator for PTC. The control limits show that each DCP accelerator has its own operating window.

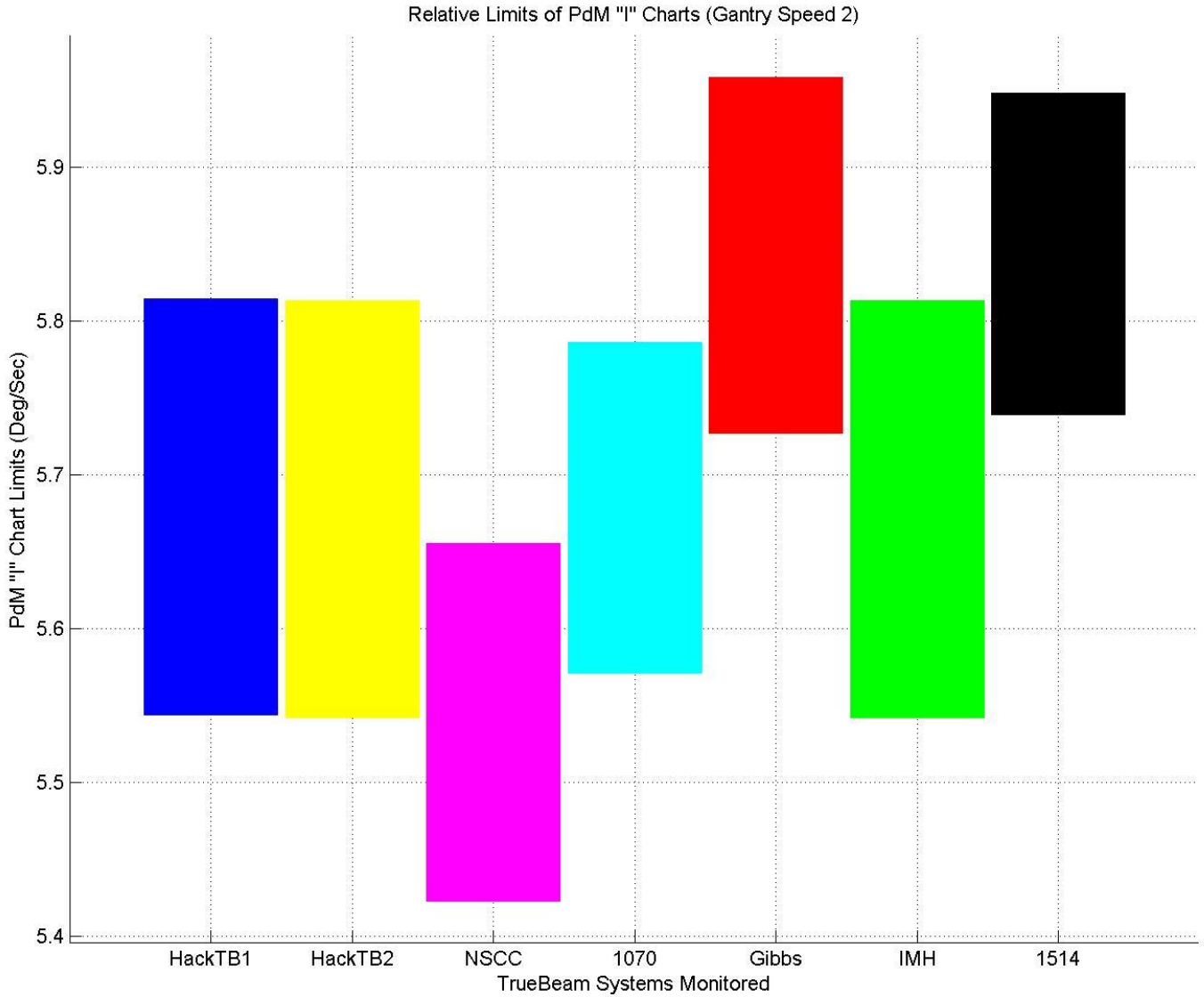

Figure 32. This figure depicts the control limits of the "I" chart for each DCP accelerator for Gantry Speed 2. The control limits show that each DCP accelerator has its own operating window.

VI. Conclusion

a. PMD Effectiveness as a PdM Tool

The PMD has shown its effectiveness as a user friendly interface displaying the PdM analysis of TrueBeam accelerator functions. The interface contains features that build an integral system for assessing degradation in performance. These features range from the status lights next to each parameter pushbutton to the visual display of chart control limits. The PMD has coded colors to alert the user of system dysfunction. Most importantly, the PMD displays the hybrid limits generated by the PdM. This allows for a graphical depiction of the behavior of each component of the TrueBeam system. All programmed features in the PMD advances PdM analytics to build an integral maintenance procedure for reducing the costs for part replacements prior to their life cycle, reducing unscheduled downtime, and strengthening the safety of radiation delivery devices.

b. PdM Reliability in Predicting Component Failure

The PdM has shown promise in identifying early detection of performance degradation in linear accelerators. PdM utilizes SPC in characterizing the behavior of processes by the use of control charts. Control charts assist in monitoring the system as a continuous process; thus, new data points can simultaneously be evaluated based on the calculated operating limit range. The modification to calculate chart control limits by using an empirical factor enhances the ability to detect deviations that result in component failure or system dysfunction. As a result, PdM detection provides an opportunity to intervene and repair the component and avoid unscheduled downtime.

c. Uniqueness of Linear Accelerator Performance

Linear accelerators are highly complex machines that consist of many subsystems. Each subsystem was found to function at a unique operating value. Performance parameters of each DCP accelerator were subjected to a ranked ANOVA. This statistical test yielded that these parameters performed at a distinct level. Graphical analysis further supported this result as the parameter means were different from each other across all DCP accelerators. Thus, linear accelerators and its components operate at distinct value, statistically and operationally. Yet, accelerators collectively meet all the clinical treatment specifications. This supports the technique that SPC is necessary to identify nonrandom changes in important performance parameters. This observation supports our hypothesis that the use of SPC provides a method to identify nonrandom changes in important performance parameters and can be used as the foundation of an accelerator PdM program.

d. Limitations

Although the PMD is a user friendly interface used in tandem with PdM analytics, it is unable to provide a true dynamic interaction with the user. A notable inability is its capacity to recognize and process when a parameter is performing in a new operating limit range. Users must supply a variable input to reset the displayed chart limits to this new range. An analytical model to adjust chart limits would be more desirable as the volume of parameters being evaluated increases. Another notable inability is its capacity to allow the user to determine a specific data point for a selected parameter. X-tick labels become clustered together, hindering the ability to determine the time of the corresponding data point.

Since SPC is a highly sensitive analysis, it has the ability to detect nonrandom behavior that is clinically relevant. Yet, it also has the capacity to identify changes that are not clinically

relevant. SPC has been effective in detecting changes in a subset of parameters; however, there are a number of parameters in which SPC has yet to detect nonrandom behavior and match the deviations to clinical importance. Long term monitoring and correlation of service interventions will be required to establish the effectiveness of SPC in linear accelerator performance.

e. Future

The PMD provides a method to detecting erratic behavior in linear accelerators. In noted instances, it has been able to predict and prevent component failure using PdM analytics. PMD materializes PdM analytics in control charts that detect nonrandom changes. It can also alert the user when successive nonrandom changes affect the overall performance of the component. Although linear accelerator performance parameters are statistically different and operate at a unique level, nonrandom changes that are present within these operating windows can be detected. The PMD is a powerful predictive maintenance tool and extensive analysis over time will better determine its overall utility.

VII. References

1. Able, C.M., et al., *Initial investigation using statistical process control for quality control of accelerator beam steering.* Radiation Oncology, 2011. **6**.
2. Able, C.M., M. Bright, and B. Frizzell, *Quality Control of High-Dose-Rate Brachytherapy: Treatment Delivery Analysis Using Statistical Process Control.* International Journal of Radiation Oncology Biology Physics, 2009. **85**(3): p. 828-833.
3. Able, C., et al., *MLC Predictive Maintenance Using Statistical Process Control Analysis.* Medical Physics, 2012. **39**(6): p. 3750-3750.
4. *Department of Defense Dictionary of Military and Associated Terms*, D.o. Defense, Editor. 2014.
5. Scheffer, C. and P. Girdhar, *Practical Machinery Vibration Analysis & Predictive Maintenance*. 2004, Burlington, MA: Newnes 252.
6. Karzmark, C.J. and R.J. Morton, *A Primer on Theory and Operation of Linear Accelerators in Radiation Therapy*. 2nd ed. 1998, Madison, WI: Medical Physics Publishing. 50.
7. Greene, D. and P.C. Williams, *Linear Accelerators for Radiation Therapy*. Second ed. Medical Science. 1997, New York, NY: Taylor & Francis Group.
8. Dyk, J.V., *The Modern Technology of Radiation Oncology* 1999, Madison, Wisconsin: Medical Physics Publishing. 1073.
9. Bjärngard, B.E. and D.A. McEwen, *Downtime experience for clinical linear accelerators.* Medical Physics, 1974. **1**(2): p. 77-78.
10. Oakland, J., *Statistical Process Control*. 2008, Jordan Hill, Oxford, UK: ButterWorth-Heinemann.
11. Stapenhurst, T., *Mastering Statistical Process Control*. 2005, Jordan Hill, Oxford, UK ButterWorth-Heinemann.
12. Wheeler, D.J. and D.S. Chambers, *Understanding Statistical Process Control*. 2nd ed. 1992, Knoxville, TN SPC Press. 401.
13. Montgomery, D., *Introduction to Statistical Quality Control*. 2005, Hoboken, New Jersey: John Wiley & Sons, Inc.
14. Able, C., A. Baydush, and C. Hampton, *Statistical Process Control Methodologies for Predictive Maintenance of Linear Accelerator Beam Quality.* Medical Physics, 2011. **38**(6): p. 3497-3497.
15. Breen, S.L., et al., *Statistical process control for IMRT dosimetric verification.* Medical Physics, 2008. **35**(10): p. 4417-4425.
16. Pawlicki, T., M. Whitaker, and A.L. Boyer, *Statistical process control for radiotherapy quality assurance.* Medical Physics, 2005. **32**(9): p. 2777-2786.
17. Pawlicki, T., et al., *Moving from IMRT QA measurements toward independent computer calculations using control charts.* Radiotherapy and Oncology, 2008. **89**(3): p. 330-337.
18. Rah, J.-E., et al., *Feasibility study of using statistical process control to customized quality assurance in proton therapy.* Medical Physics, 2014. **41**(9).
19. *Manual on Quality Control of Materials*. American Society for Testing and Materials 1951, Philadelphia, PA, USA.
20. Burr, I.W., *The effect of non-normality on constants for X-bar and R charts.* Industrial Quality Control 1996. **23**(11): p. 563-568.

21. Neubauer, D.V., *Manual on Presentation of Data and Control Chart Analysis*. 8th ed. 2010, West Conshohocken, PA: ASTM International. 97.
22. Van Esch, A., et al., *Implementing RapidArc into clinical routine: A comprehensive program from machine QA to TPS validation and patient QA.* Medical Physics, 2011. **38**(9): p. 5146-5166.
23. *MATLAB and Statistics Toolbox Release 2013a*. 2013, The Mathworks, Inc. : Natick, Massachusetts, United States.
24. Able, C. and A. Baydush, *Effective Control Limits for Predictive Maintenance (PdM) of Accelerator Beam Uniformity.* Medical Physics, 2013. **40**(6): p. 1.
25. Able, C., C. Hampton, and A. Baydush, *Flatness and Symmetry Threshold Detection Using Statistical Process Control.* Medical Physics, 2012. **39**(6): p. 3751-3751.
26. Bai, S., et al., *Effect of MLC leaf position, collimator rotation angle, and gantry rotation angle errors on intensity-modulated radiotherapy plans for nasopharyngeal carcinoma.* Medical Dosimetry, 2013. **38**(2): p. 143-147.
27. Haga, A., et al., *Dose verification of volumetric modulated arc therapy (VMAT) by use of in-treatment linac parameters.* Radiological physics and technology, 2013. **6**(2): p. 335-42.
28. Klein, E.E., et al., *Task Group 142 report: Quality assurance of medical accelerators.* Medical Physics, 2009. **36**(9): p. 4197-4212.
29. Kutcher, G.J., et al., *COMPREHENSIVE QA FOR RADIATION ONCOLOGY - REPORT OF AAPM RADIATION-THERAPY COMMITTEE TASK-GROUP-40.* Medical Physics, 1994. **21**(4): p. 581-618.
30. Shoales, J. and A. Boyer, *Multi-leaf collimator quality assurance using pulse width modulation analysis.* Medical Physics, 2007. **34**(6): p. 2474-2474.
31. Conover, W.J. and R.L. Iman, *Rank Transformations as a Bridge Between Parametric and Nonparametric Statistics.* The American Statistician, 1981. **35**(3): p. 124-129.

VIII. Scholastic Vita

Callistus I Huy Minh Nguyen

CONTACT INFORMATION

170 Crowne Chase Dr., Apartment 12
Winston Salem, NC 27104
canguyen@wakehealth.edu
(919)-332-4605 – cell

EDUCATION

Virginia Tech – Wake Forest School of Biomedical Engineering and Sciences **August 2012 – Present**
Ph.D, Biomedical Engineering, Expected May 2017
Cumulative GPA: 3.55

Virginia Tech – Wake Forest School of Biomedical Engineering and Sciences **August 2012 – December 2014**
M.S., Biomedical Engineering, December 2014
Cumulative GPA: 3.55

Wake Forest University
B.S. Biophysics, Minor in Chemistry, December 2010
Cumulative GPA: 3.3 Major GPA: 3.6

PROFESSIONAL EXPERIENCE

Virginia Tech – Wake Forest School of Biomedical Engineering and Sciences **August 2012 – Present**
Radiation Oncology, Wake Forest School of Medicine, Winston Salem, NC
Graduate Student

- **TrueBeam Predictive Maintenance (PdM): Statistical Process Quality Control of RapidArc Performance Parameters:** Assisted in the design of the Statistical Process Control (SPC) database of linear accelerator parameters. Developed an interface to display, manage, and report SPC results of all parameters in the database. Determined the effectiveness of I/MR tests to detect performance dysfunction.

Virginia Tech - Wake Forest School of Biomedical Engineering and Sciences **February 2011 – August 2012**
Center for Injury Biomechanics, Winston Salem, NC
Research Intern

- **Rib Morphology:** Segmented and registered ribs from Computed Tomography (CT) scans of male and female subjects aged 0-100 years to gather landmarks for morphological analysis. Landmarks gathered are used to generate shape and size functions and develop models to predict chest injury.
- **Skull Morphology:** Segmented Computed Topography scans of skulls to generate point clouds representing the skull surface needed for modeling and analysis of the human skull.
- **Volumetric Analysis of Lung Injury:** Registered lung lobes from the Crash Injury Research Engineering Network (CIREN) database to a lung altas to determine the location of injured tissue in an atlas based coordinate system.
- **Hip Morphology:** Collected 2D angular measurements for normal and Femoroacetabular Impingements (FAI) hips. Gathered hip rim profiles for the quantification of the morphology of the acetabular rim profile and comparison of differences in hips that have Femoroacetabular Impingements.
- **Sternum Morphology:** Developed and improved an algorithm to segment and register CT scans of male and female subjects aged 0-100 years to collect landmark data to quantify age and gender-specific variations in morphology

Biophysics and Nanotechnology Research Group, **August 2007 – December 2010**
Wake Forest University, Winston Salem, NC
Undergraduate Research Assistant

- Researched the changes in radii of fibrin fibers as a function of various conditions.
- Determined the compliance of fibrin fibers was related to the Hertz equation.
- Extracted the Young's modulus of fibrin fibers and compared this value to other elastic materials.

FOREIGN STUDY

Wake Forest-Vietnam Summer Study Abroad Program **July 2009 – August 2009**

- Explored the impact of entrepreneurship and social entrepreneurship on Vietnamese society.
- Analyzed the major ways in which politics and economics systems were organized in Vietnam.
- Participated in a service project in Rach Gia, Vietnam and reinvigorated the children's desire to attend school.

HONORS/AWARDS

Wake Forest Travel Alumni Award (Fall 2014)
Southeast American Association of Physicists in Medicine Symposium – Best Student Poster (Spring 2014)
Wake Forest University Research Fellowship (Summer 2008 and Summer 2009)
Wake Forest University Deans List (6 of 8 Undergraduate Semesters)

COMPUTING SKILLS

MATLAB, Mimics, 3DSlicer, Geomagic Studio 12, Paint Shop Pro 7, ImageJ, Aquarius NetClient and iNtuition,

PROFESSIONAL MEMBERSHIPS

Biomedical Engineering Society (BMES), VT-WFU Chapter	2014 – Present
American Association of Physicists in Medicine (AAPM)	2014 – Present
Radiation Research Society (RRS)	2014 – Present

BIBLIOGRAPHY

Papers in Refereed Journals

Weaver AA, Schoell SL, **Nguyen CM**, Lynch SK, Stitzel JD. "Morphometric Analysis of Variation in the Sternum with Sex and Age," **Journal of Morphology**, 2014 Nov; 275(11):1284-99. doi: 10.1002/jmor.203002

Weaver AA, **Nguyen CM**, Schoell SL, Maldjian JA, Stitzel JD, "Image segmentation and registration algorithm to collect thoracic skeleton landmarks for age and sex characterization," **Biomed Research International,** Sept 2014 *(In review)*

Able CM, Baydush AH, **Nguyen CM**, Gersh J, Ndlovu A, Rebo I, Booth J, Perez M, Sintay B, Munley MT, "A Model for Pre-emptive Maintenance of Medical Linear Accelerators: Predictive Maintenance," **International Journal of Radiation Oncology**, 2014 Sept; 90(1): S738. doi: 10.1016/j.ijrobp.2014.05.2147

Papers in Refereed Conference Publications

Weaver AA, **Nguyen CM**, Schoell SL, Stitzel JD. "Morphological Analysis of Changes in the Thoracic Skeleton with Age and Gender," **2nd International Digital Modeling Symposium**. June 2013.

Other Conference Papers (abstract style or non-refereed)/Scientific Exhibits

Able CM, **Nguyen CM**, Baydush AH, Gersch J, Ndlovu A, Rebo I, Booth J, Perez M, Sintay B, Munley MT, "Predictive Maintenance of Medical Accelerators: A Customized Dashboard Interface," **Radiological Society of North America**, Chicago, IL, November 2014.

Nguyen CM, Able CM, Baydush AH, Munley MT. "Development of a Predictive Maintenance GUI for Medical Linear Accelerators," **Biomedical Engineering Society Annual Meeting**, Austin, TX, October 2014.

Weaver AA, Schoell SL, Nguyen CM, Stitzel JD. "Morphological analysis of changes in the thoracic skeleton with sex and age." **Biomedical Engineering Society Annual Meeting**, Austin, TX, October 2014.

Weaver AA, Schoell SL, Nguyen CM, Stitzel JD. "Morphological analysis of changes in the thoracic skeleton with sex and age." **World Congress Biomechanics**, Boston, MA, July 2014.

Able CM, Baydush AH, **Nguyen CM**, Gersch J, Ndlovu A, Rebo I, Booth J, Perez M, Sintay B, Munley MT, "Effective Analysis of VMAT QA Generated Trajectory Log Files for Medical Accelerator Predictive Maintenance," **American Association of Physicists In Medicine Annual Meeting and Exhibition**, San Antonio, TX, July 2014.

Able CM, Baydush AH**, Nguyen CM**, Gersch J, Ndlovu A, Rebo I, Booth J, Perez M, Sintay B, Munley MT, "Analysis of Accelerator Generated Text Logs for Preemptive Maintenance," **American Association of Physicists In Medicine Annual Meeting and Exhibition**, San Antonio, TX, July 2014.

Nguyen CM, Able CM, Baydush AH, Munley MT. "Development of a Predictive Maintenance GUI for Medical Linear Accelerators," **Virginia Tech – Wake Forest University School of Biomedical Engineering and Sciences Graduate Research Symposium**, Winston Salem, NC, May 2014.

Nguyen CM, Able CM, Baydush AH, Munley MT. "Development of a Predictive Maintenance GUI for Medical Linear Accelerators," **Southeast American Association of Physicists in Medicine Symposium and Scientific Meeting**, Chattanooga, TN, May 2014.

Weaver AA, **Nguyen CM**, Schoell SL, Stitzel JD. "Morphological Analysis of Changes in the Thoracic Skeleton with Age and Gender," **Virginia Tech – Wake Forest University School of Biomedical Engineering and Sciences Graduate Research Symposium,** Blacksburg, VA, May 2013.

Weaver AA, **Nguyen CM**, Schoell SL, Maldjian JA, Stitzel JD, "Image segmentation and registration algorithm to collect thoracic skeleton landmarks for age and sex characterization," **Computer Methods in Biomechanics and Biomedical Engineering**. February 2013.

Weaver AA, **Nguyen C**, Wyatt CL, Stitzel JD. "Quantifying Rib Morphology Across Ages and Genders Using Image Segmentation and Registration Techniques," **Biomedical Engineering Society Annual Meeting**, Hartford, CT, October 2011.

Weaver AA, **Nguyen C**, Stitzel JD. "Quantification of Sternal Morphology Across Ages and Genders Using Image Segmetnation and Registration Techniques," **ASME 2012 Summer Bioengineering Conference**, Fajardo, Puerto Rico, USA, June 2012.